ENERGETIC-PARTICLE-DRIVEN INSTABILITIES: LINEAR PHYSICS NEAR THE THRESHOLD

S.E. Sharapov

UKAEA, Culham Science Centre, Abingdon OX14 3DB, UK

OUTLINE

- INTRODUCTION: ALFVÉN INSTABILITIES IN BURNING DT PLASMA
- MHD DESCRIPTION OF ALFVÉN WAVES IN PLASMA
- THE ISSUE OF CONTINUUM DAMPING AND DISCOVERY OF GLOBAL ALFVÉN EIGENMODES
- TOROIDAL ALFVÉN EIGENMODES: THEORY, QUALITATIVE ESTIMATES, AND EXPERIMENT
- NEAR-THRESHOLD DYNAMICS OF TAE IN THE “SOFT” INSTABILITY CASE
- SUMMARY

INTRODUCTION

ALFVÉN INSTABILITIES IN BURNING DT PLASMA

- α-particles (He^4 ions) are born in D-T nuclear reactions with birth energy 3.52 MeV exceeding plasma temperature ~100 times
- For typical B and n, velocities of α-particles exceed Alfvén velocity, $V_A=B/(4\pi\rho)^{1/2}$, so that

$$V_{Ti} << V_A < V_\alpha << V_{Te}$$

- During their slowing-down, α-particles cross the Alfvén wave resonance

$$V_A = V_{\|\alpha}$$

  and may excite Alfvén instabilities
- Free energy source for such instabilities is radial pressure gradient of α's.
- The instability results in a radial re-distribution / loss of α-particles if the amplitude of the Alfvén wave becomes high
- Present-day machines with ICRH/ NBI excite Alfvén instabilities very often

ALFVÉN INSTABILITIES SEEN EASILY FROM δB PERTURBATIONS

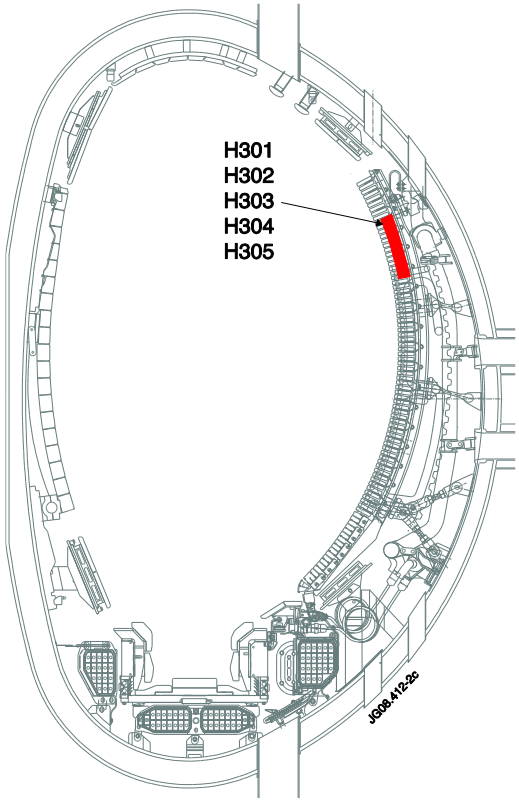

JET tokamak: a cross-section showing the position and directivity of Mirnov coils

- **Mirnov coils are used for measuring perturbed magnetic flux just outside the plasma:**

$$\frac{\partial}{\partial t}\delta B_{\vartheta}^{edge} \cong \omega \cdot \delta B_{\vartheta}^{edge}$$

- **The coils are VERY sensitive for high frequencies, e.g. for values of $\omega \cong 10^{6}\ \ \mathrm{sec}^{-1}$ perturbed fields $\left|\delta B_{\vartheta}^{edge} / B_{0}\right| \cong 10^{-8}$ are measured**

Typical measurements have the frequencyrange of 500 kHz – 1 MHz

TYPICAL DATA SHOWS *DISCRETE* SPECTRUM OF ENERGETIC PARTICLE-DRIVEN ALFVÉN WAVES

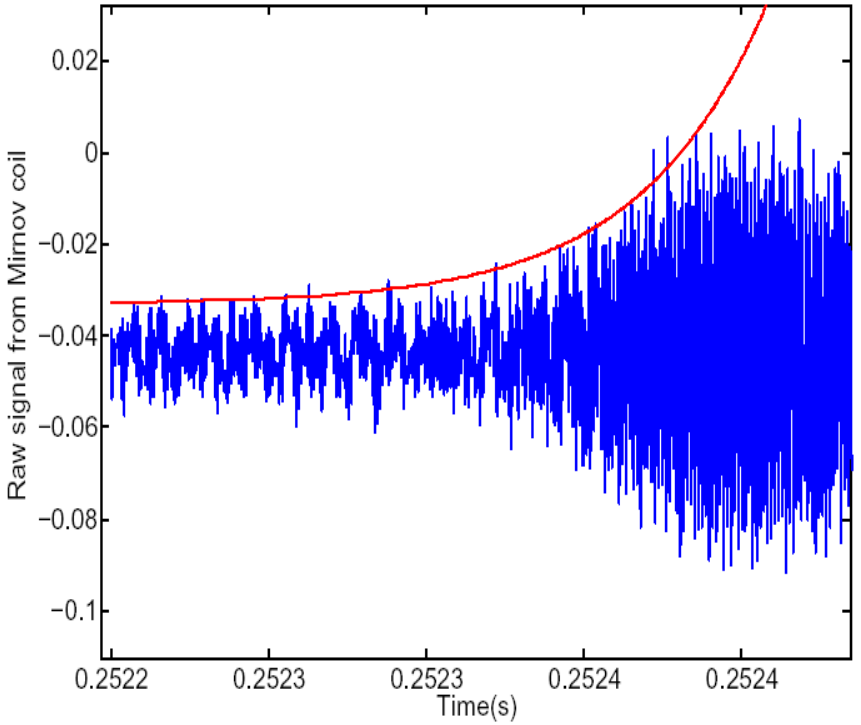

Raw data from a Mirnov coil just outside the plasma

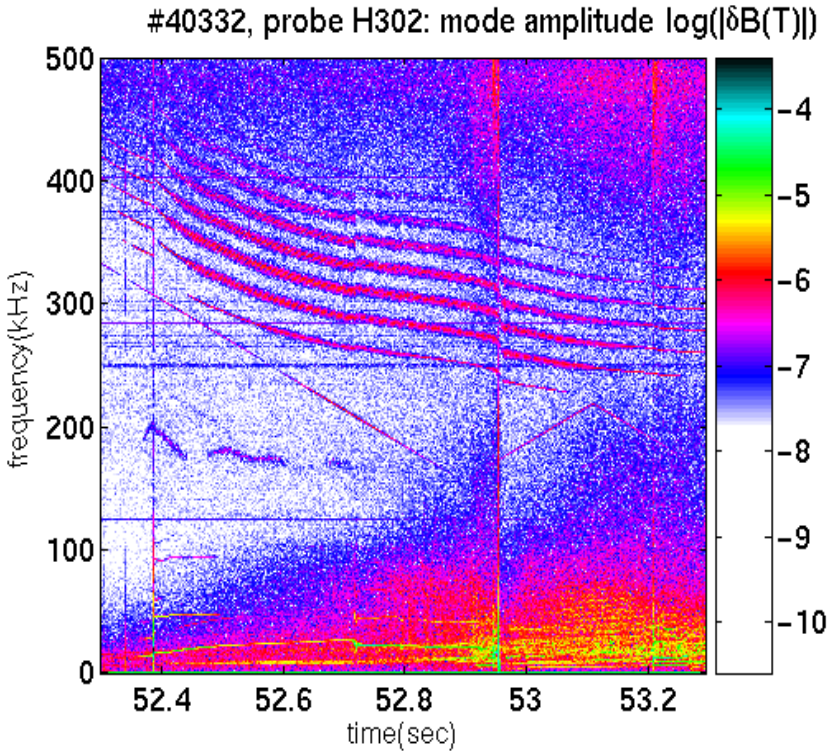

Typical magnetic spectrogram of Mirnov signal from plasma with energetic particles

MOST OF THE DATA TO BE SHOWN IS FROM TOKAMAK JET (JOINT EUROPEAN TORUS)

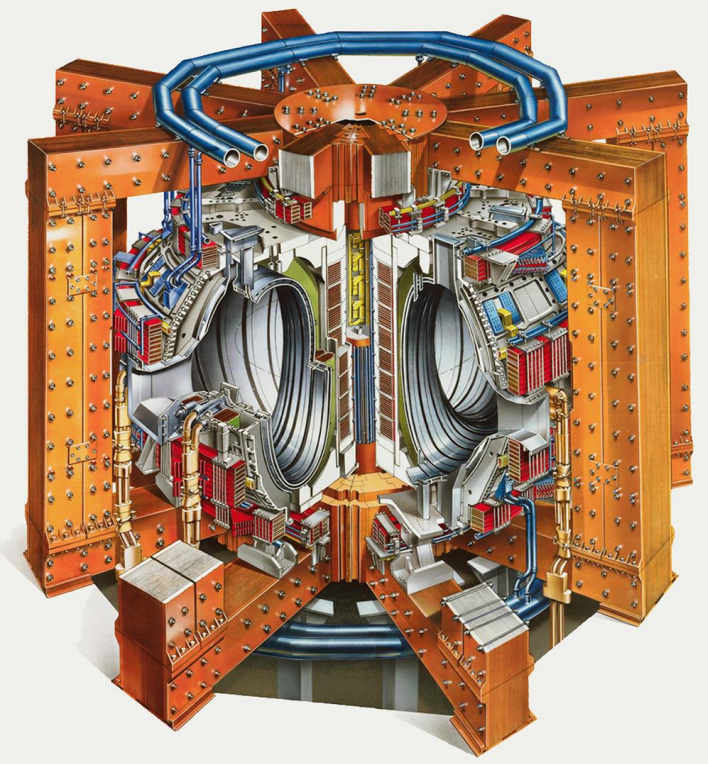

Volume ~ 100 m^3; B_{max} = 4 T; I_{max} = 7 MA; P_{FUS} = 16 MW

ENERGETIC IONS IN JET VERSUS EXPECTED ALPHAS IN ITER

Machine	JET	JET	JET	JET	ITER
Type of fast ions	Hydrogen	He^3	He^4	Alpha	Alpha
Source	ICRH tail	ICRH tail	ICRH tail	Fusion	Fusion
Mechanism	minority	minority	3rd harm. NBI	DT nuclear	DT nuclear
$V_f(0)/V_A(0)$	≈2	≈1.5	≈1.3	1.6	1.9
τ_S (s)	1.0	0.9	0.4	1.0	0.8
P_f (0) (MW/m^3)	0.8	1.0	0.5	0.12	0.55
n_f (0) / n_e (0) (%)	1.0	1.5	1.5	0.44	0.85
β_f (0) (%)	2	2	3	0.7	1.2
$\langle\beta_f\rangle$ (%)	0.25	0.3	0.3	0.12	0.3
max$\lvert R\beta'_f \rvert$ (%)	≈5	≈5	5	3.5	3.8

Ratio of on-axis velocities $V_f(0)/V_A(0)$, slowing down time, τ_S , heating power per volume, P_f (0), ratio of the fast ion density to electron density, n_f (0) / n_e (0), on-axis fast ion beta, β_f (0), volume-averaged fast ion beta, $\langle\beta_f\rangle$, and normalised radial gradient of fast ion beta, max| Rβ'$_f$ |, in JET vs. ITER projected parameters.

THE ALFVÉN WAVES OBSERVED:

WHY THEY ARE SEEN IN PLASMAS WITH ENERGETIC PARTICLES ONLY?

WHY THEY FORM A DISCRETE SPECTRUM?

HOW TO DESCRIBE THEM AND HOW IMPORTANT THEY ARE FOR BURNING PLASMA MACHINES?

MHD DESCRIPTION OF ALFVÉN WAVES IN PLASMA

STARTING MAGNETO-HYDRODYNAMIC (MHD) EQUATIONS FOR ELECTROMAGNETIC WAVES IN MAGNETISED PLASMAS

- For describing ***plasma particles***, we take velocity moments of the kinetic equations for thermal electron and thermal ion distribution functions and obtain

$$\frac{\partial \rho}{\partial t} + \nabla \cdot (\rho \mathbf{V}) = 0 ;$$

$$\rho \frac{d\mathbf{V}}{dt} = -\nabla p + \frac{1}{c} \mathbf{J} \times \mathbf{B} ;$$

$$\frac{\partial p}{\partial t} + \mathbf{V} \cdot \nabla p + \gamma \ p \nabla \cdot \mathbf{V} = 0 ;$$

$$\mathbf{E} + \frac{1}{c} \mathbf{V} \times \mathbf{B} = 0 ;$$

- For describing ***electromagnetic fields*** in the plasma, Maxwell's equations are used

$$\nabla \times \mathbf{B} = \frac{4\pi}{c} \mathbf{J}$$

$$\nabla \times \mathbf{E} = -\frac{1}{c} \frac{\partial \mathbf{B}}{\partial \mathbf{t}}$$

$$\nabla \cdot \mathbf{B} = 0$$

- Here, scale lengths larger than Debye length are considered with $n_e = \sum_i Z_i \cdot n_i$

THE LINEARISATION PROCEDURE

- All the field and plasma variables are represented as sums of equilibrium (denoted by subscript 0) and perturbed (denoted by δ) quantities:

$$\mathbf{J} = \mathbf{J}_0 + \delta\mathbf{J}\,,\ \mathbf{B} = \mathbf{B}_0 + \delta\mathbf{B}\,,\ \mathbf{V} = \delta\mathbf{V}\,,\ p = p_0 + \delta p\,,\ \rho = \rho_0 + \delta\rho\,,\ \mathbf{E} = \delta\mathbf{E}\,, \qquad (*)$$

  where all the perturbed quantities satisfy $\delta << 1$, i.e. $|\delta\mathbf{J}/\mathbf{J}_0| << 1$ etc.

- Substitute the expressions (*) in the starting set of equations and obtain equations with terms: a) not having δ at all; b) having δ; c) having δ^2 etc.

- The terms NOT having δ are balanced thanks to the plasma equilibrium

$$\nabla p_0 = \frac{1}{c}\mathbf{J}_0 \times \mathbf{B}_0$$

  The relation between equilibrium quantities $\mathbf{J}_0,\ p_0,\ B_0$ MUST be kept in all equations with δ

- All the equations are linearised then, i.e. only linear terms in δ are kept and terms with δ^2 etc. are dropped off as small (since $\delta << 1$)

LINEARISED MHD EQUATIONS

- **The linearised ideal MHD equations take the form:**

$$\frac{\partial \delta\rho}{\partial t} + \nabla\cdot\left(\rho_0 \delta\mathbf{V}\right) = 0 ;$$

$$\rho_0 \frac{d\delta\mathbf{V}}{dt} = -\nabla\delta p + \frac{1}{4\pi}\left[\nabla\times\delta\mathbf{B}\right]\times\mathbf{B}_0 ;$$

$$\frac{\partial}{\partial t}\delta\mathbf{B} = \nabla\times\left[\delta\mathbf{V}\times\mathbf{B}_0\right];$$

$$\delta p = \gamma\ \frac{p_0}{\rho_0}\delta\rho ;$$

- **Introduce *plasma displacement* from the equilibrium, ξ, which is related to $\delta\mathbf{V}$ via**

$$\delta\mathbf{V} = \partial\boldsymbol{\xi}/\partial t$$

- **From the first and third equations we find then**

$$\delta\rho = -div\left(\rho_0\boldsymbol{\xi}\right);\ \ \delta\mathbf{B} = \nabla\times\left[\boldsymbol{\xi}\times\mathbf{B}_0\right] = -\mathbf{B}_0 div\boldsymbol{\xi}_\perp + \mathbf{B}_0\frac{\partial\boldsymbol{\xi}_\perp}{\partial z}$$

where we used $\nabla\times\left[\mathbf{a}\times\mathbf{b}\right] = \left(\mathbf{b}\nabla\right)\mathbf{a} - \left(\mathbf{a}\nabla\right)\mathbf{b} + \mathbf{a}\ div\mathbf{b} - \mathbf{b}\ div\mathbf{a}$ **, and** $\mathbf{B}_0 \uparrow\uparrow \mathbf{e}_z$

EQUATION FOR IDEAL MHD WAVES

- **Substitute the expressions for $\delta\rho$, $\delta\mathbf{B}$ in the remaining two equations and obtain**

$$\frac{\partial^2 \boldsymbol{\xi}}{\partial t^2} = c_S^2 \nabla div\boldsymbol{\xi} + V_A^2 \nabla_\perp div\boldsymbol{\xi}_\perp + V_A^2 \frac{\partial^2 \boldsymbol{\xi}_\perp}{\partial z^2},$$

Where $c_S^2 = \gamma\ p_0 / \rho_0$ is the ion sound speed, $V_A^2 = B_0^2 / (4\pi\rho_0)$ is the Alfvén velocity

- **This equation describes *linear MHD perturbations of homogeneous ideally conducting plasma*. Single vector equation gives three scalar equations for *three types of waves***

PLASMA DISPLACEMENT IN MHD WAVES

- ***Compressional Alfvén and slow magnetosonic waves:*** **the "returning" force is the magnetic and the kinetic pressure**

- ***Shear Alfvén wave:*** **the "returning" force is the tension of magnetic field lines**

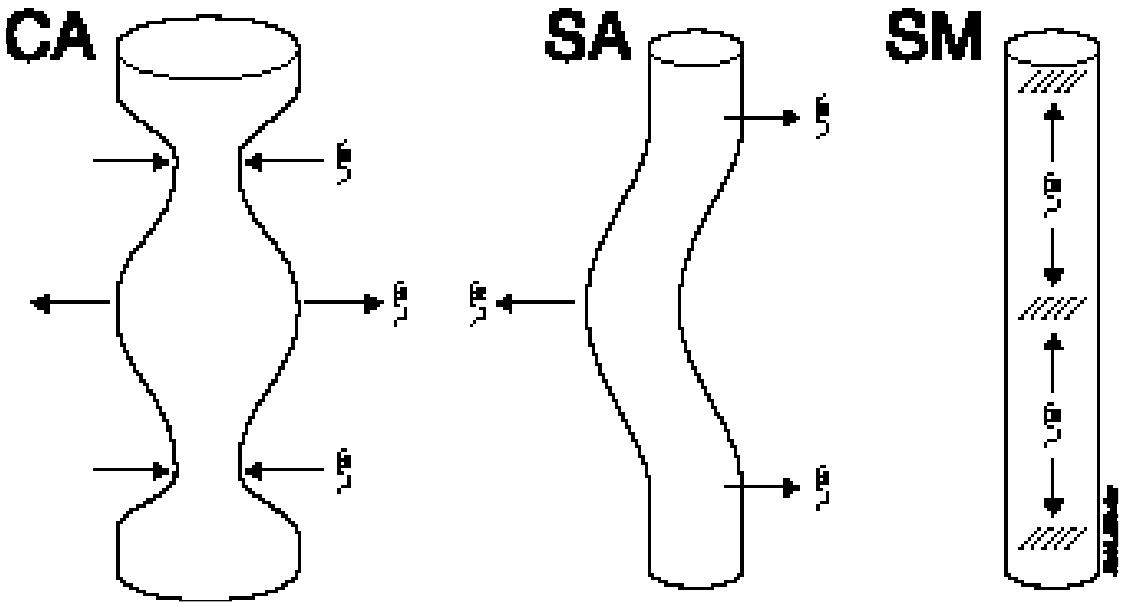

SHEAR ALFVÉN WAVES

- **In contrast to the compressional waves, *Shear Alfvén wave* is *incompressible*:**

$$\xi_z = 0 \text{ and } div\boldsymbol{\xi}_\perp = 0$$

- **For such waves the main MHD equation becomes**

$$\frac{\partial^2 \boldsymbol{\xi}_\perp}{\partial t^2} = V_A^2 \frac{\partial^2 \boldsymbol{\xi}_\perp}{\partial z^2}$$

which coincides with equation, e.g., for string oscillations. The "returning" force is the tension of magnetic field lines, which acts similarly to the strings

- **In such shear Alfvén wave the fluid displacement vector $\boldsymbol{\xi}$ and $\tilde{\mathbf{E}}$ are perpendicular to the magnetic field $\mathbf{B}_0$. The wave propagates along $\mathbf{B}_0$:**

$$\omega = \pm k_\parallel V_A \text{ ; } V_A = \frac{B_0}{\sqrt{4\pi \sum_i n_i M_i}} \text{ ; } \quad k_\parallel = \mathbf{k} \cdot \mathbf{B}_0 / B_0$$

- **Among all the waves in plasmas, the Alfvén wave (*H. Alfvén, Arkiv. Mat. Astron. Fysik 29B(2) (1942)*) constitutes the most significant part of the MHD spectrum and is probably the best studied**

THE ISSUE OF CONTINUUM DAMPING AND DISCOVERY OF GLOBAL ALFVÉN EIGENMODES

ALFVÉN WAVE PERTURBATION IN *INHOMOGENEOUS* PLASMA

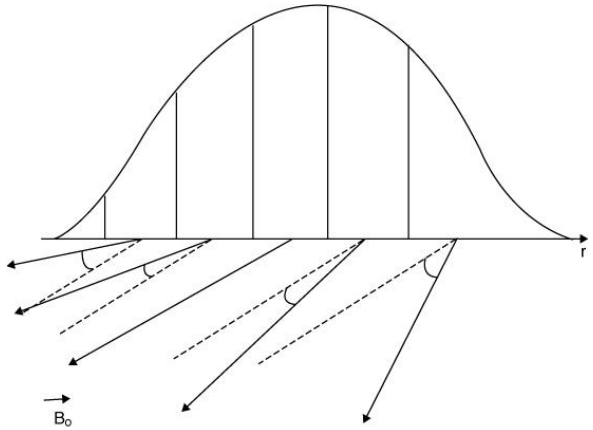

$$\omega = k_{\parallel}(r)\cdot V_A(r)$$

The life-time τ of a radially-extended shear Alfvén perturbation is short due to the "phase mixing" between different modes forming Alfvén continuum

$$\tau^{-1} \propto \frac{d}{dr}\left(k_{\parallel}(r)\cdot V_A(r)\right),$$

This could be interpreted as the wave continuum "damping rate" $\gamma_d \approx \tau^{-1}$.

τ could be long if the wave is localised at the extremum point of Alfvén continuum,

$$\frac{d}{dr}\left(k_{\parallel}(r)\cdot V_A(r)\right)=0$$

ANTENNA-DRIVEN WAVE IN INHOMOGENEOUS PLASMA-1

- **Consider 1-D slab non-uniform cold plasma,** $n_0 = n_0(x)$, $P_0 = 0$, $\mathbf{B}_0 = B_0 \mathbf{e}_Z$,

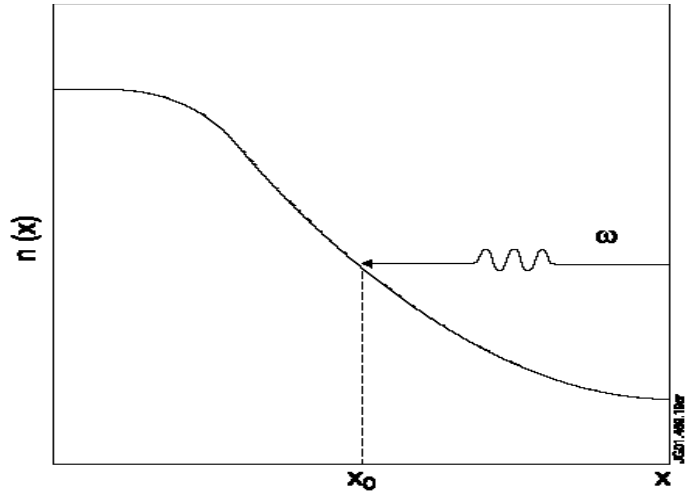

- **The presence of *plasma gradients* modifies our MHD equation. An externally excited electromagnetic wave with perturbed** $\phi \propto \phi(x)\exp(ik_y y - i\omega t)$ **is described by**

$$\frac{d}{dx}\left(\omega^2 - \omega_A^2(x)\right)\frac{d\phi}{dx} - k_y^2\left(\omega^2 - \omega_A^2(x)\right)\phi = 0$$

$$\omega_A^2(x) \equiv k_\parallel^2 V_A^2(x)$$

ANTENNA-DRIVEN WAVE IN INHOMOGENEOUS PLASMA - 2

- **This equation has *zero coefficient at high order derivative at the point* $x = x_0$ of the local Alfvén resonance layer, where**

$$\omega^2 = \omega_A^2(x_0)$$

- **Investigating the equation in the vicinity of this point:**

$$\frac{d}{dx}\left(\omega^2 - \omega_A^2(x)\right)\frac{d\phi}{dx} = 0 \;\rightarrow\; \frac{d\phi}{dx} = \frac{const}{\omega^2 - \omega_A^2(x)}$$

- **Expand the local Alfvén frequency in the vicinity of the point $x = x_0$:**

$$\omega^2 = \omega_A^2(x_0) + d\omega_A^2(x)/dx\Big|_{x=x_0} \cdot (x - x_0)$$

and obtain

$$\phi \propto const \cdot \ln(x - x_0), \quad x > x_0$$

$$\phi \propto const \cdot \left(\ln|x - x_0| + i\pi\right), \quad x < x_0$$

The *wave energy peaks up at* $x = x_0$ and resonant absorption of the wave energy occurs at this point

LINEAR MODE CONVERSION TO KINETIC ALFVÉN WAVE

- **Finite ion Larmor radius & finite electron parallel conductivity incorporated in the layer $|x - x_0| \approx \rho_i$ remove the wave singularity**
- **Wave equation takes the form $(m_e / M_i << \beta_e << 1)$:**

$$\omega^2 \rho_i^2 \nabla_\perp^2 \left(\frac{3}{4}(1 - i\delta_i) + \frac{T_e}{T_i}(1 - i\delta_e) \right) \nabla_\perp^2 \phi + + \frac{d}{dx}\left(\omega^2 - \omega_A^2(x)\right)\frac{d\phi}{dx} - k_y^2 \left(\omega^2 - \omega_A^2(x)\right)\phi = 0$$

- **Solution of this equation satisfies the dispersion relation in the form of Kinetic Alfvén Wave:**

$$\omega^2 = k_\parallel^2 V_A^2(x) \left(1 + (k_x \rho_i)^2 \left(\frac{3}{4}(1 - i\delta_i) + \frac{T_e}{T_i}(1 - i\delta_e) \right) \right)$$

- **In contrast to the shear Alfvén wave, KAW propagates across $\mathbf{B}_0$, $\partial \omega_{KAW} / \partial k_x \neq 0$, and it has $\tilde{E}_\parallel \neq 0$**

LINEAR MODE CONVERSION TO KINETIC ALFVÉN WAVE

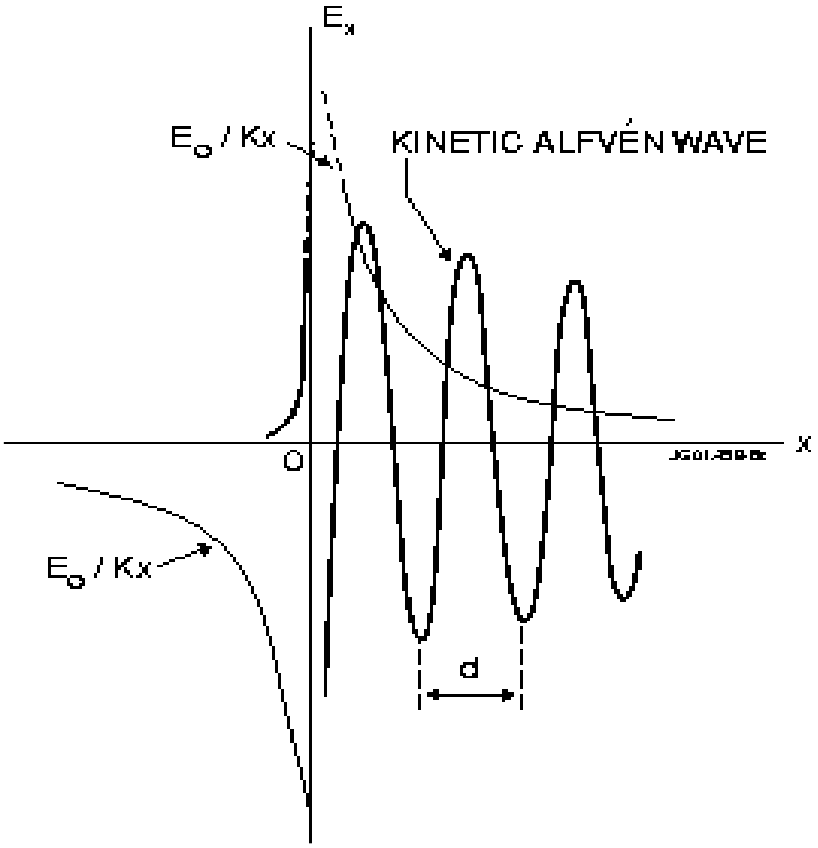

DO ANY SHEAR ALFVÉN MODES EXIST WHICH DO NOT SATISFY A LOCAL SA DISPERSION RELATION AND ARE FREE OF THE CONTINUUM DAMPING?

DISCOVERY OF GLOBAL ALFVÉN EIGENMODE

- **In cylindrical geometry, in addition to the continuous Alfvén spectrum, $\omega^2 = \omega_A^2(r) \equiv k_\parallel^2(r) V_A^2(r)$, a discrete Global Alfvén Eigenmode with frequency $\omega_{GAE} < \omega_A$ exists in plasma with current (*D.W.Ross et al. Phys. Fluids 25, 652 (1982);K.Appert et al. Plasma Phys. 24, 1147 (1982)*)**

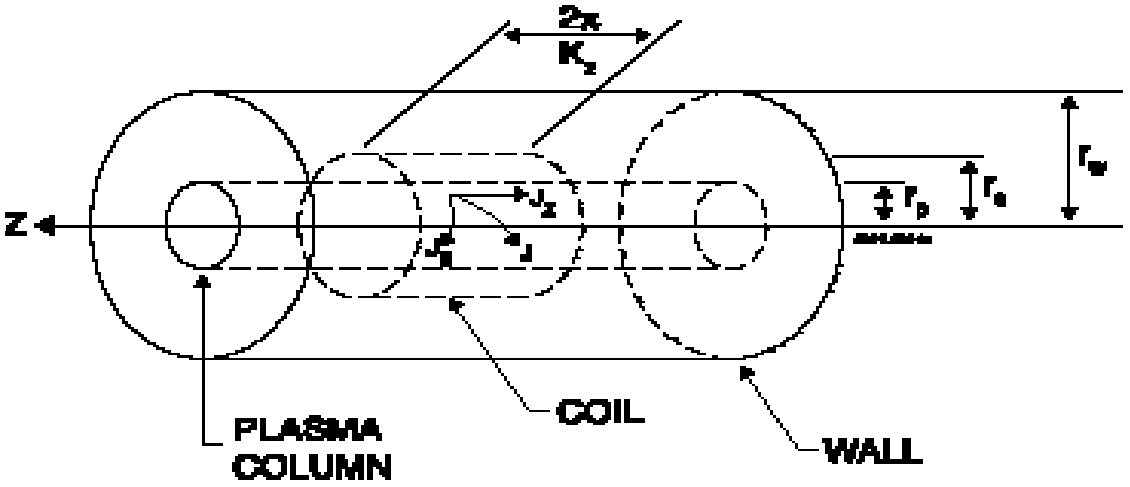

The ideal plasma-coil-wall system used in the numerical investigation

DISCOVERY OF GLOBAL ALFVÉN EIGENMODE

- **A new high-quality, $Q \equiv \omega/\gamma \sim 10^3$, resonance was discovered during these Alfvén antenna studies, in plasmas with current**

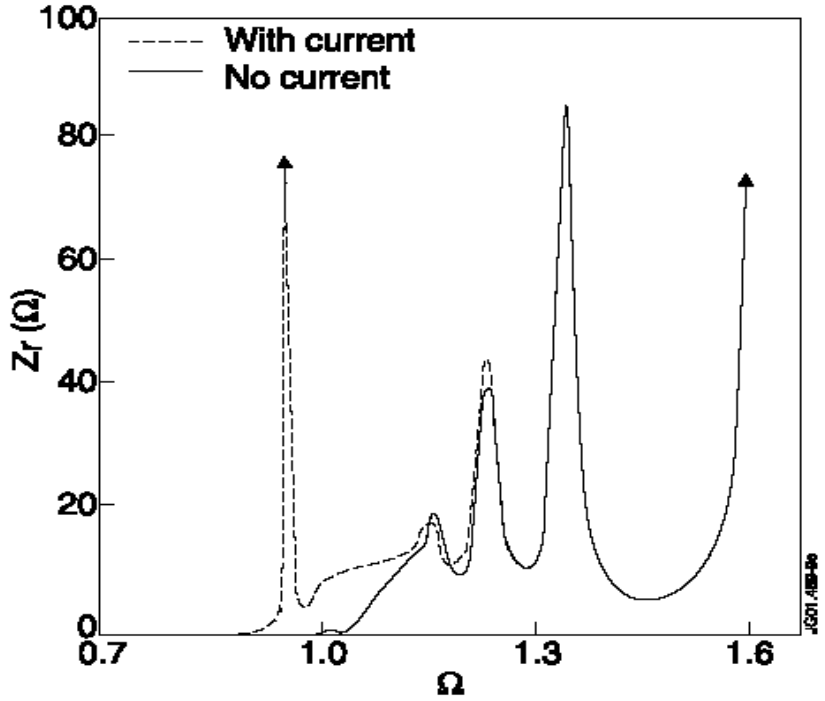

Real part of the coil impedance vs normalized frequency

GLOBAL ALFVÉN EIGENMODE

- **GAE with $\omega_{GAE} < \omega_A$ exists in Ideal MHD if the current profile determining dB_ϑ / dr provides a minimum in Alfvén continuum**

$$\left.\frac{d\omega_A(r)}{dr}\right|_{r=r_0} = 0 \text{, i.e. } \frac{1}{k_\parallel}\frac{dk_\parallel}{dr} = -\frac{1}{V_A}\frac{dV_A}{dr}$$

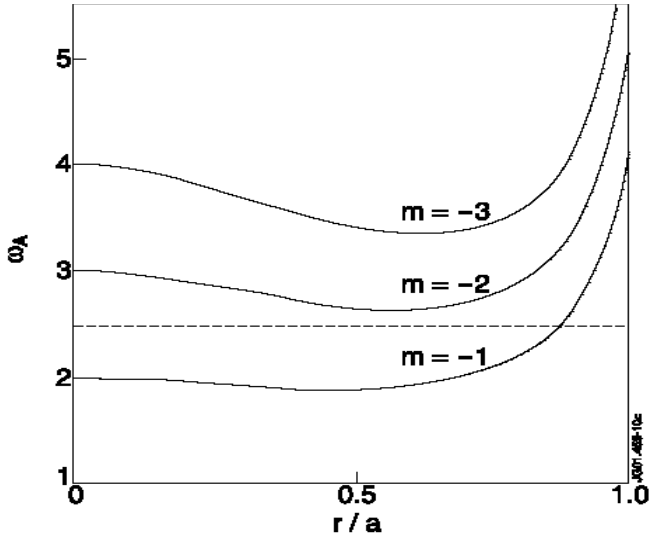

- **The local minimum of the Alfvén continuum provides a *maximum of the perpendicular refraction index* $N_r = ck_r / \omega$. Similarly to fiber optics, the *electromagnetic wave* has to propagate in a *"wave-guide" surrounding the region of the extremum refraction index.***

NO CONTINUUM DAMPING FOR GLOBAL ALFVÉN EIGENMODE

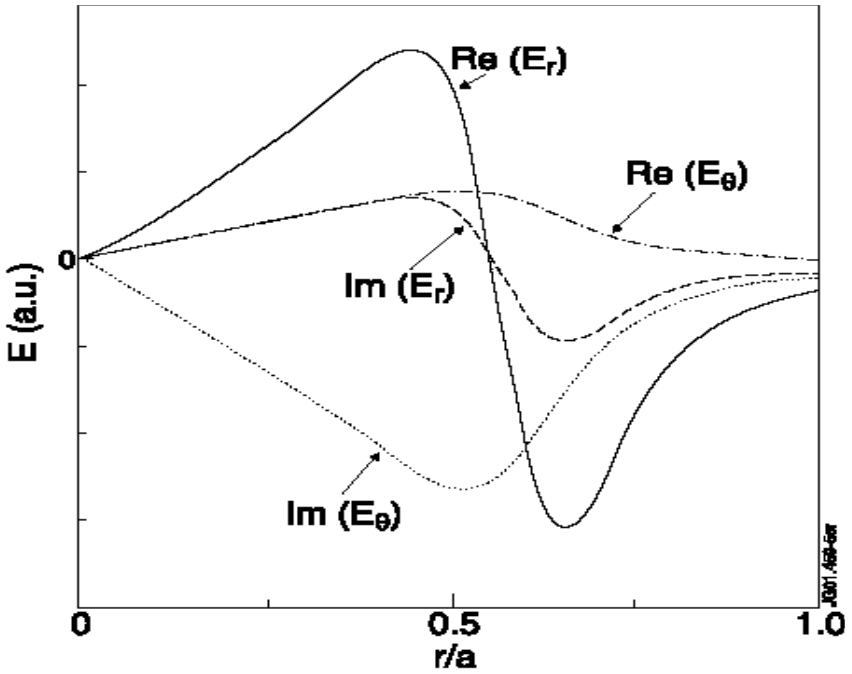

Ideal MHD GAE with m=-2

- **The eigenfrequency of GAE does *not* satisfy the local Alfvén resonance condition, $\omega_{GAE} \neq \omega_A(r)$, for $0 < r/a < 1$. Therefore, this SA mode has *no* singularity and does *not* experience *continuum damping***

ANOTHER TYPE OF ALFVÉN MODE THAT DOES NOT EXPERIENCE HIGH CONTINUUM DAMPING: TOROIDAL ALFVÉN EIGENMODE (TAE)

THE PARALLEL WAVE-VECTOR IN TOKAMAK

In a torus, the wave solutions are quantized in toroidal and poloidal directions:

$$\phi(r,\vartheta,\zeta,t)=\exp\left(-i\omega\ t+in\zeta\right)\sum_m \phi_m(r)\ \exp\left(-im\vartheta\right)+c.c.$$

n is the number of wavelengths in toroidal direction and
m is the number of wavelengths in poloidal direction

- **The parallel wave-vector for the m-th harmonic of a mode with toroidal mode number n,**

$$k_{\|m}(r)=\frac{1}{R}\left(n-\frac{m}{q(r)}\right),$$

is determined by the safety factor $q(r)=rB_\zeta / RB_\vartheta$.

- **For a given $q(r)$ and n, one finds $m=nq$ giving a rational surface with $k_{\|m}=0$**
- **This also gives $\omega_A(r)=k_{\|m}(r)V_A(r)=0$ and the "gap" $0<\omega<\omega_A$ cannot exist, in contrast to cylindrical geometry**

RADIAL STRUCTURE OF ALFVÉN CONTINUUM IN TOKAMAK

Due to the poloidal dependence of equilibrium parameters, e.g.

$$B = B_0\left(1-\left(r/R\right)\cos\vartheta\right),$$

where

$$\cos\vartheta = \left(e^{i\vartheta}+e^{-i\vartheta}\right)/2$$

poloidal m-th and (m+1)-th harmonics of a perturbation couple to form a "toroidicity-induced gap" in the Alfvén continuum at the frequency satisfying

$$\omega = k_{\|m}(r)V_A(r) = -k_{\|m+1}(r)V_A(r)$$

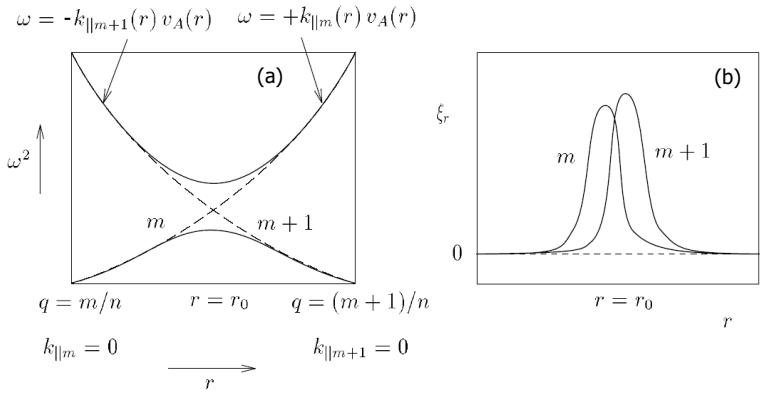

A discrete eigenmode with frequency inside this gap exists and is called Toroidicity-induced Alfvén Eigenmode (TAE)

WHY TAE-GAP EXISTS?

- **The coupled set of differential equations**

$$\frac{\partial}{\partial r}\left(\frac{\omega^2}{v_A^2}-k_{\|m}^2\right)\frac{\partial\phi_m}{\partial r}-\frac{m^2}{r^2}\left(\frac{\omega^2}{v_A^2}-k_{\|m}^2\right)\phi_m+\frac{\epsilon}{4q^2R_0^2}\frac{\partial^2\phi_{m-1}}{\partial r^2}=0$$

$$\frac{\partial}{\partial r}\left(\frac{\omega^2}{v_A^2}-k_{\|m-1}^2\right)\frac{\partial\phi_{m-1}}{\partial r}-\frac{m^2}{r^2}\left(\frac{\omega^2}{v_A^2}-k_{\|m-1}^2\right)\phi_{m-1}+\frac{\epsilon}{4q^2R_0^2}\frac{\partial^2\phi_m}{\partial r^2}=0$$

has to have *zero determinant at higher order derivatives* → gap in frequency

$$\left(\frac{\omega^2}{v_A^2}-k_{\|m}^2\right)\cdot\left(\frac{\omega^2}{v_A^2}-k_{\|m-1}^2\right)-\frac{\epsilon^2}{16q^4R_0^4}=0$$

WHY TAE-GAP EXISTS?

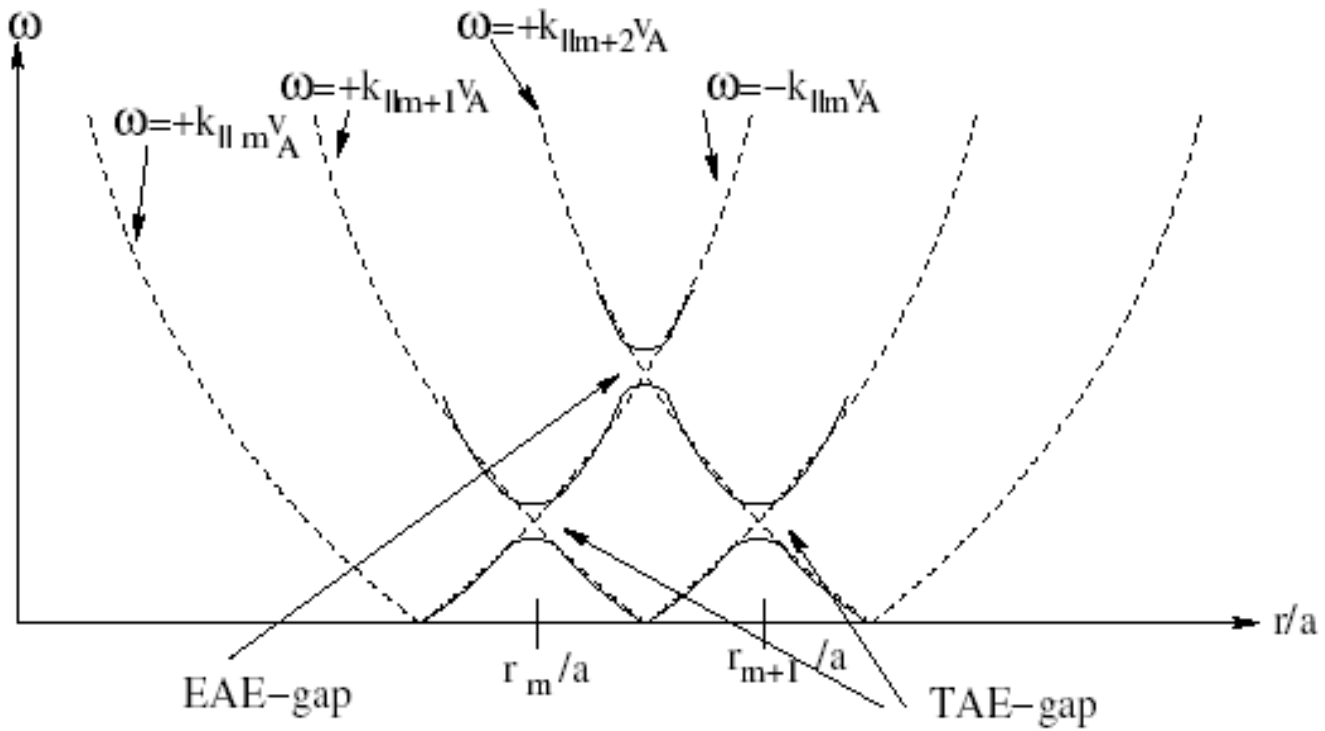

- **In fact, higher order gaps also exist associated with Ellipticity, Triangularity etc.**

HOW TO OBTAIN DISCRETE TAE ANALYTICALLY?

- **Limit of small magnetic shear is the best case**
- **Introduce operator**

$$L_m\phi_m \equiv \frac{d}{dr}\left(\frac{\omega^2}{v_A^2} - k_{\|m}^2\right)\frac{d\phi_m}{dr} - \frac{m^2}{r^2}\left(\frac{\omega^2}{v_A^2} - k_{\|m}^2\right)\phi_m$$

and re-write the coupled equations

$$L_m\phi_m + \epsilon\frac{1}{4q^2R^2}\frac{d^2\phi_{m-1}}{dr^2} = 0$$

$$L_{m-1}\phi_{m-1} + \epsilon\frac{1}{4q^2R^2}\frac{d^2\phi_m}{dr^2} = 0$$

- **Consider two regions, one far away from the extremum point (outer region exactly like in cylindrical geometry) and one – in the vicinity of the extremum point (inner region)**

HOW TO OBTAIN DISCRETE TAE ANALYTICALLY?

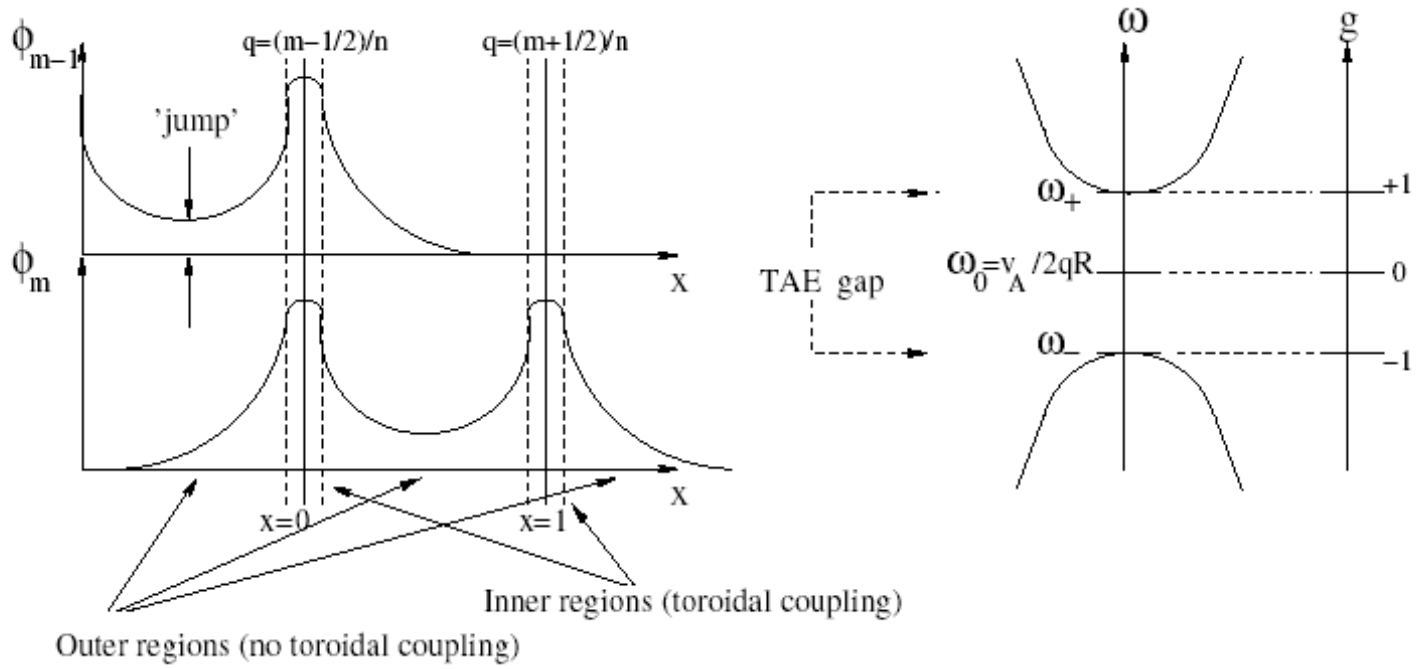

$$g = \frac{1}{\epsilon}\left(\omega^2\left(\frac{2qR}{v_A}\right)^2 - 1\right) \Leftrightarrow \frac{\omega^2}{v_A^2} = \frac{1}{4q^2R^2}(1+\epsilon g)$$

HOW TO OBTAIN DISCRETE TAE ANALYTICALLY?

- **In the Inner region, the equations can be directly integrated to give**

$$\phi_m^{in} = \frac{C_m}{2}\ln|z^2+(1-g^2)| - \frac{gC_m + C_{m-1}}{(1-g^2)^{1/2}}\tan^{-1}\left(\frac{z}{(1-g^2)^{1/2}}\right) + const$$

$$\phi_{m-1}^{in} = \frac{C_{m-1}}{2}\ln|z^2+(1-g^2)| + \frac{C_m + gC_{m-1}}{(1-g^2)^{1/2}}\tan^{-1}\left(\frac{z}{(1-g^2)^{1/2}}\right) + const$$

where

$$z = \frac{4}{\epsilon}(nq(r) - m + 1/2)$$

- **The solution has some "jumps" in electrostatic potential:**

$$\Delta\phi_m^{in} = \phi_m^{in}(z\to+\infty) - \phi_m^{in}(z\to-\infty) = -\frac{gC_m + C_{m-1}}{(1-g^2)^{1/2}}\left(+\frac{\pi}{2} - \left(-\frac{\pi}{2}\right)\right)$$

$$= -\pi\frac{gC_m + C_{m-1}}{(1-g^2)^{1/2}}$$

$$\Delta\phi_{m-1}^{in} = \ldots = \pi\frac{C_m + gC_{m-1}}{(1-g^2)^{1/2}}$$

HOW TO OBTAIN DISCRETE TAE ANALYTICALLY?

- **These jumps must be compensated by opposite jumps in the "outer" solution, thus giving TAE dispersion equation**

$$C_m = C_{m-1}\ ; \quad g = \ldots = \frac{-1+\frac{\pi^2 S^2}{16}}{1+\frac{\pi^2 S^2}{16}} \cong -\left(1-\frac{\pi^2 S^2}{16}\right)^2 \cong -1+\frac{\pi^2 S^2}{8}$$

Fpr details see, e.g. B.N.Breizman and S.E. Sharapov, PPCF 1057 (1995)

RADIAL STRUCTURE OF ALFVÉN CONTINUUM AND TAE IN JET

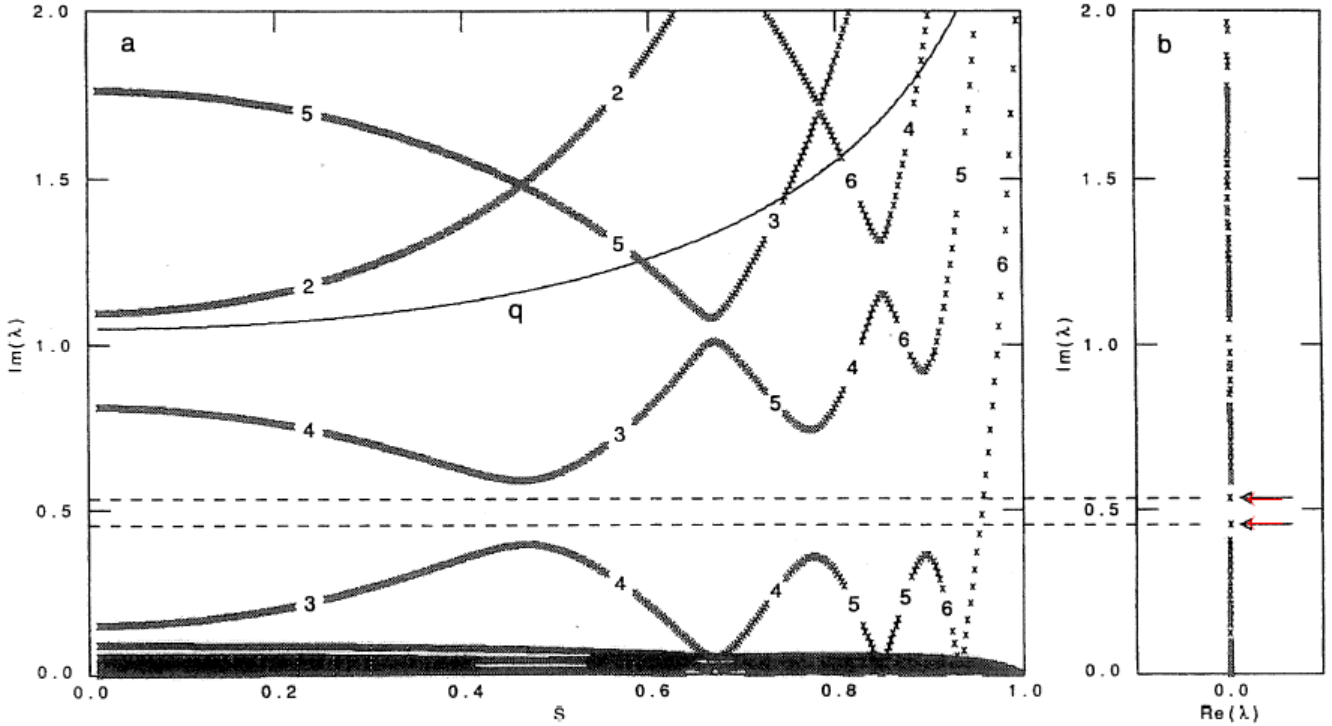

Typical structure of Alfvén continuum (and SM continuum) in toroidal geometry

Numerous extremum points $\left.\frac{d\omega_A(r)}{dr}\right|_{r=r_0}=0$ exist providing the necessary conditions for many TAEs to be supported by the toroidal equilibrium!

RADIAL MODE STRUCTURE OF TAE

- **Similarly to GAE in cylinder, TAE frequency does not satisfy local Alfvén resonance condition in the region of TAE localization, $\omega_{TAE} \neq \omega_A(r)$, so TAE has no singularity and does not experience strong continuum damping**

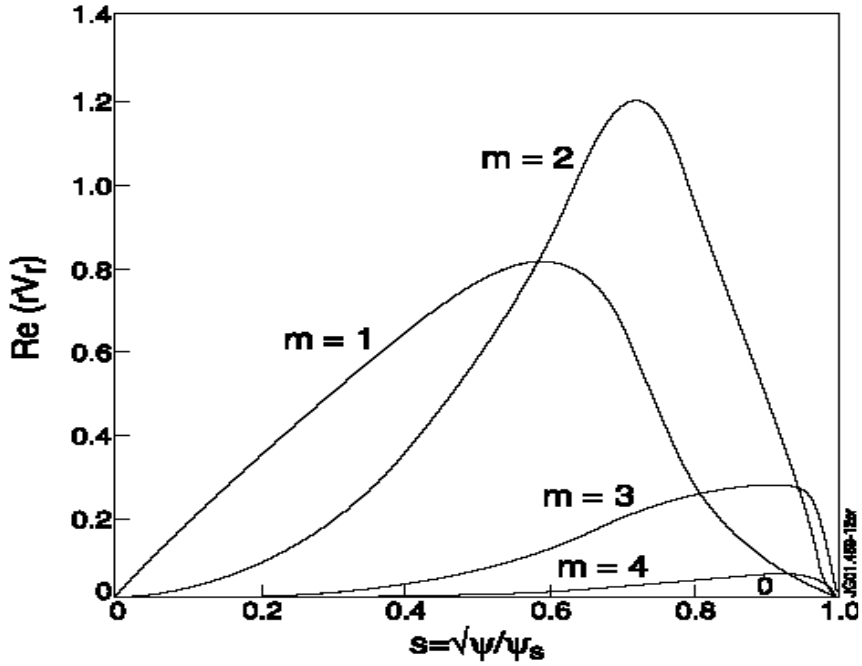

Radial dependence of the Fourier harmonics of TAE

TAE OBSERVATIONS VIA MAGNETIC SENSORS (MIRNOV COILS)

CHARACTERISTIC PROPERTIES OF TAE -1

- **Gap in the Alfvén continuum appears in toroidal geometry at frequency**

$$\omega = k_{\|m}(r)V_A(r) = -k_{\|m+1}(r)V_A(r)$$

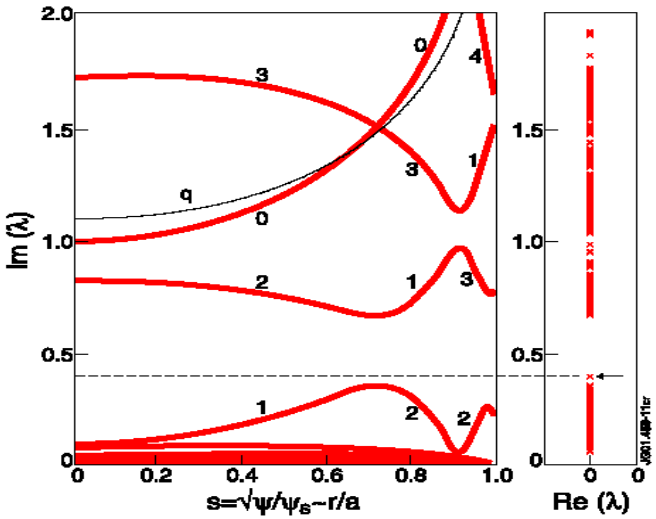

Ideal MHD continuous spectrum of n=1, m=0,1,2,3,4

Shear Alfvén and SM frequencies versus $s = \sqrt{\psi_p / \psi_p^{edge}} \propto r/a$

- **In addition to the continuum, Toroidal Alfvén Eigenmodes (TAEs) exist in the TAE gaps**

CHARACTERISTIC PROPERTIES OF TAE - 2

- **Start from the TAE-gap condition** $\omega = k_{\|m}(r)V_A(r) = -k_{\|m+1}(r)V_A(r)$ **(*)**

$$\downarrow$$

$$k_{\|m}(r) = -k_{\|m+1}(r)$$

$$\downarrow$$

$$\frac{1}{R_0}\left(n - \frac{m}{q(r)}\right) = -\frac{1}{R_0}\left(n - \frac{m+1}{q(r)}\right)$$

$$\downarrow$$

$$q(r) = \frac{m+1/2}{n}$$

- **TAE gap is localised at** $q(r_0) = (m+1/2)/n$ **determined by the SA values of** n **and** m
- **Substitute this value of safety factor in the starting equation (*) to obtain**

$$\omega_0 = \frac{V_A(r_0)}{2R_0 q(r_0)}$$

CHARACTERISTIC PROPERTIES OF TAE - 3

- **Localisation of TAE gaps determined by** $q(r_0) = (m + 1/2)/n$ **for typical** $0.75 < q < 5$ **are:**

	m=1	m=2	m=3	m=4	m=5	m=6
n=1	1.5	2.5	3.5	4.5	5.5	6.5
n=2	0.75	1.25	1.75	2.25	2.75	3.25
n=3	0.5	0.83	1.167	1.5	1.83	2.167
n=4		0.625	0.875	1.125	1.375	1.625
n=5		0.5	0.7	0.9	1.1	1.3
n=6			0.583	0.75	0.917	1.083

- **Characteristic frequencies of the TAE gap for JET parameters are:**

$$B_0 \cong 3\ T\ ;\ n_i = 5\times 10^{19}\ \ m^{-3}\ ;\ m_i = m_D$$

$$\downarrow$$

$$V_A \cong 6.6\times 10^6\ \ m/s$$

- **For typical value of q=1.1 one has the frequency estimate then:**

$$\omega_0 \cong 10^6\ \ \sec^{-1} \rightarrow \qquad f_0 \equiv \omega_0 / 2\pi \cong 160\ \ kHz$$

HOW TO DETECT SHEAR ALFVÉN WAVES?

Looking for wave solutions in torus, which are quantized in toroidal and poloidal directions:

$$\phi(r,\vartheta,\zeta,t) = \exp\left(-i\omega\, t + in\zeta\right) \sum_m \phi_m(r)\ \exp\left(-im\vartheta\right) + c.c.$$

n **is the number of wavelengths in toroidal direction and** m **is the poloidal mode number**

- **The parallel wave-vector for the** m **-th harmonic of a mode with toroidal mode number** n **,**

$$k_{\parallel m}(r) = \frac{1}{R}\left(n - \frac{m}{q(r)}\right), \qquad q(r) = rB_\zeta / RB_\vartheta$$

- ***Shear Alfvén waves*** **with perturbed scalar** ϕ **and vector** $\delta\mathbf{A}$ **potentials satisfy:**

$$\delta B_\parallel \equiv \delta\mathbf{B}\cdot\mathbf{B}_0 / B_0 = 0 \ \rightarrow\ \delta\mathbf{A} = \delta A_\parallel \left(\mathbf{B}_0 / B_0\right) \equiv \delta A_\parallel\, \mathbf{b}$$

$$\delta E_\parallel \equiv \delta\mathbf{E}\cdot\frac{\mathbf{B}_0}{B_0} = 0 = -\mathbf{b}\cdot\nabla\phi - \frac{1}{c}\frac{\partial}{\partial t}\delta A_\parallel \ \rightarrow\ k_\parallel\,\phi = \frac{\omega}{c}\delta A_\parallel$$

- **Express perturbed m-th perpendicular electric and magnetic fields now:**

$$\delta E_r = -\frac{\partial\phi_m}{\partial r}\exp\left(i\left[n\zeta - m\vartheta - \omega t\right]\right) + c.c. \qquad \delta E_\vartheta = \frac{im}{r}\phi_m \exp\left(i\left[n\zeta - m\vartheta - \omega t\right]\right) + c.c.$$

$$\delta B_r = -\frac{k_\parallel c}{\omega}\cdot\frac{im}{r}\phi_m \exp\left(i\left[n\zeta - m\vartheta - \omega t\right]\right) + c.c. \qquad \delta B_\vartheta = -\frac{k_\parallel c}{\omega}\cdot\frac{\partial\phi_m}{\partial r}\exp\left(i\left[n\zeta - m\vartheta - \omega t\right]\right) + c.c.$$

MIRNOV COILS

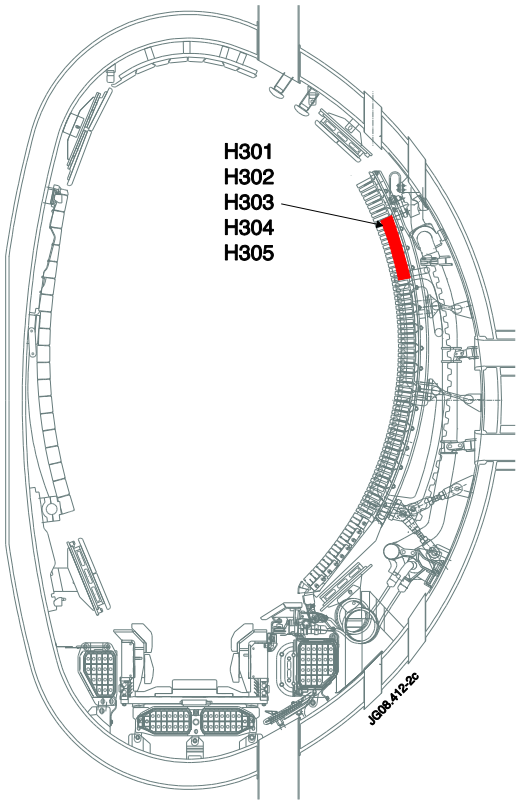

JET cross-section showing the position and directivity of five Mirnov coils separated in toroidal angle

- **Mirnov coils for measuring magnetic flux due to δB_ϑ are best performing on JET**
- **The coils measure**

$$\frac{\partial}{\partial t}\delta B_\vartheta^{edge} \cong \omega \cdot \delta B_\vartheta^{edge}$$

and are VERY sensitive! Thanks to high values of $\omega \cong 10^6 \ \sec^{-1}$ perturbed fields $\left|\delta B_\vartheta^{edge} / B_0\right| \cong 10^{-8}$ are measured

- **Sampling rate 1 MHz allows measurements of AE up to 500 kHz to be made**

A MIRNOV COIL RAW DATA

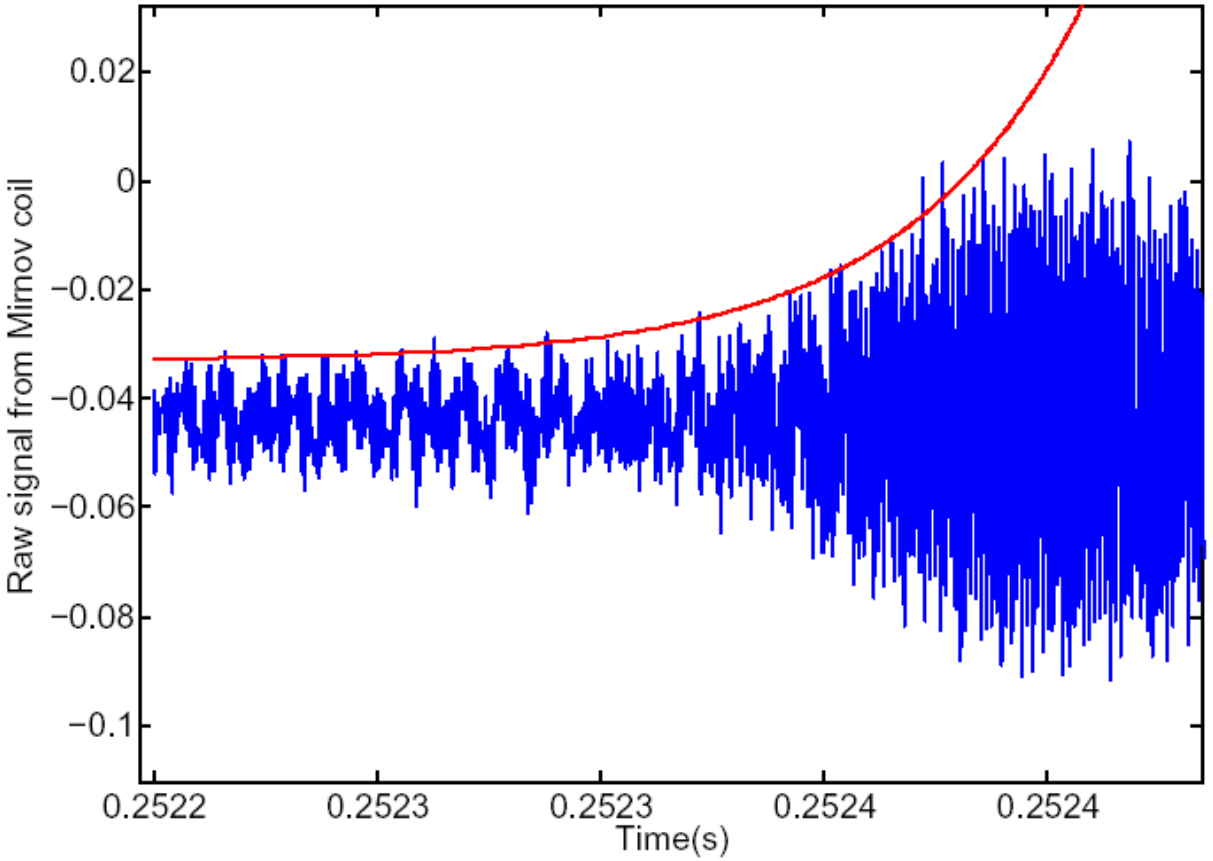

How to extract any useful information from this?

FOURIER TRANSFORMED DATA – AMPLITUDE SPECTROGRAM

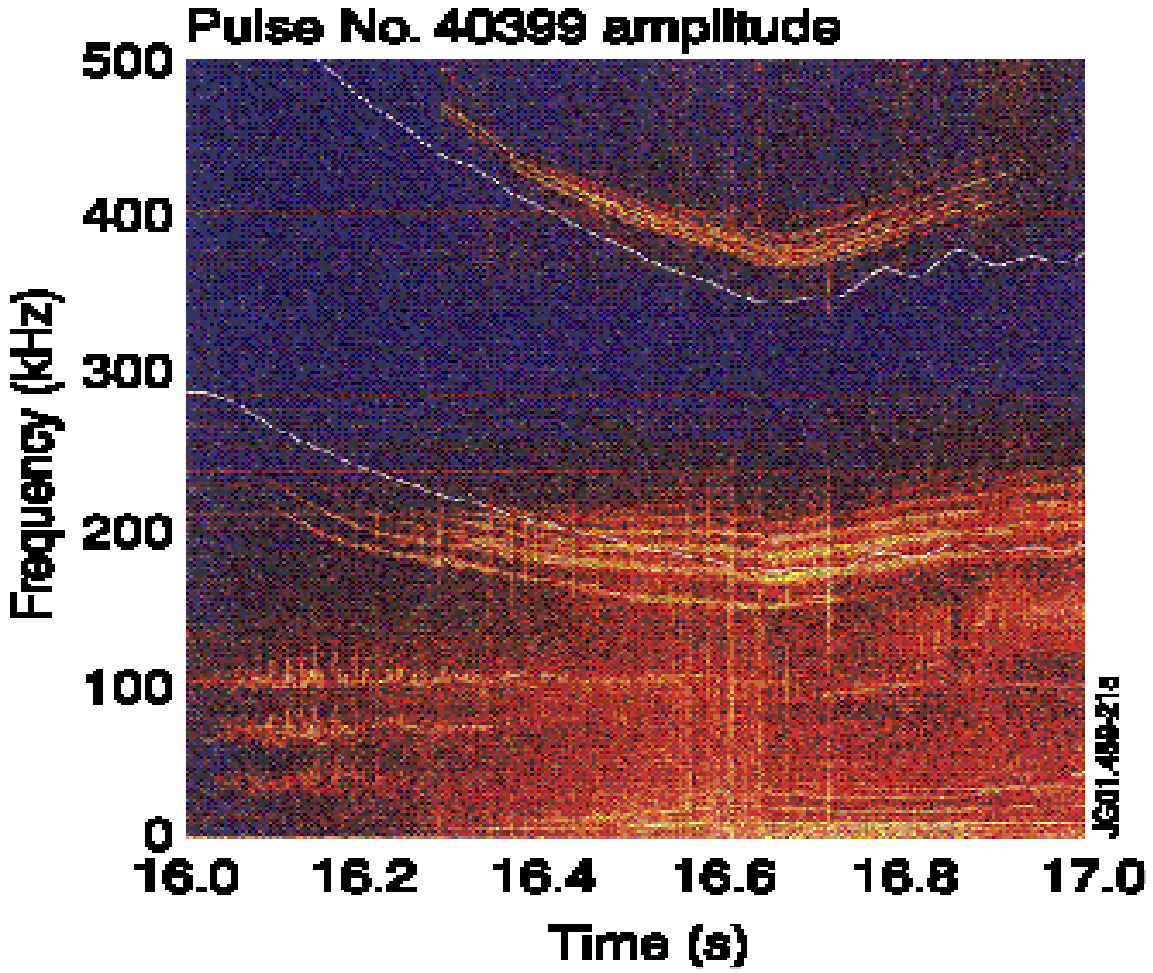

SET OF MIRNOV COILS PROVIDE ALSO THE *PHASE* DATA

- **For determining toroidal mode number of the mode, phase shift is measured between two (or more) Mirnov coils at different toroidal angles**

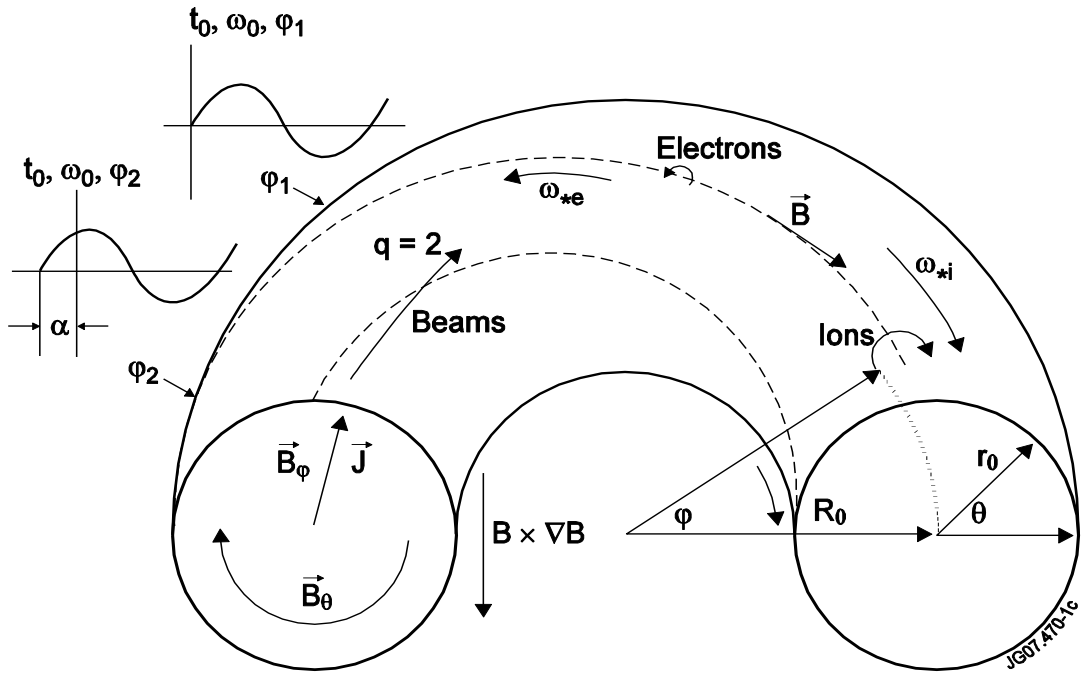

Sinusoidal signals measured at different toroidal angles at the same time and at same frequency are shifted in phase by α.

FOURIER TRANSFORMED DATA – PHASE SPECTROGRAM

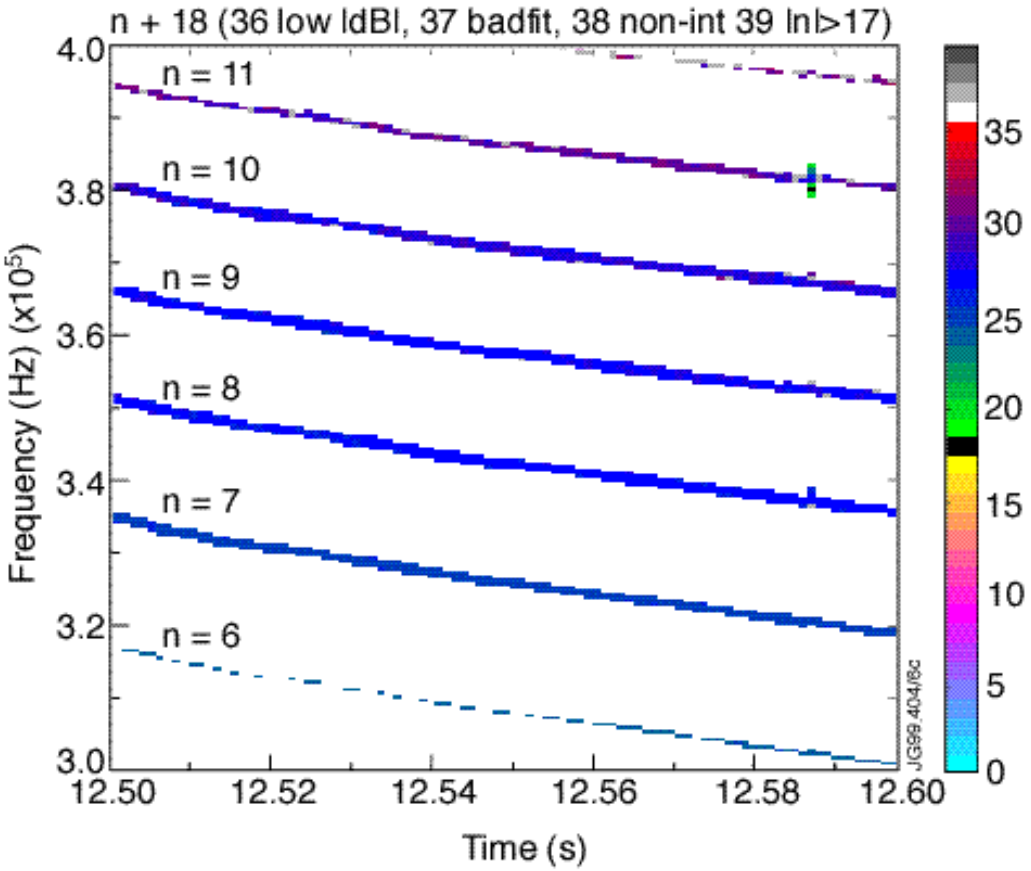

THE NYQUIST UNDER - SAMPLING EFFECT - 1

If a function $x(t)$ contains no frequencies higher than B cycles per second, it is completely determined by giving its ordinates at a series of points spaced $1/(2B)$ seconds apart.

See, e.g.

C. E. Shannon, *Communication in the presence of noise*, Proc. Institute of Radio Engineers **37**, 10 (1949).

THE NYQUIST UNDER - SAMPLING EFFECT IN AMPLITUDE

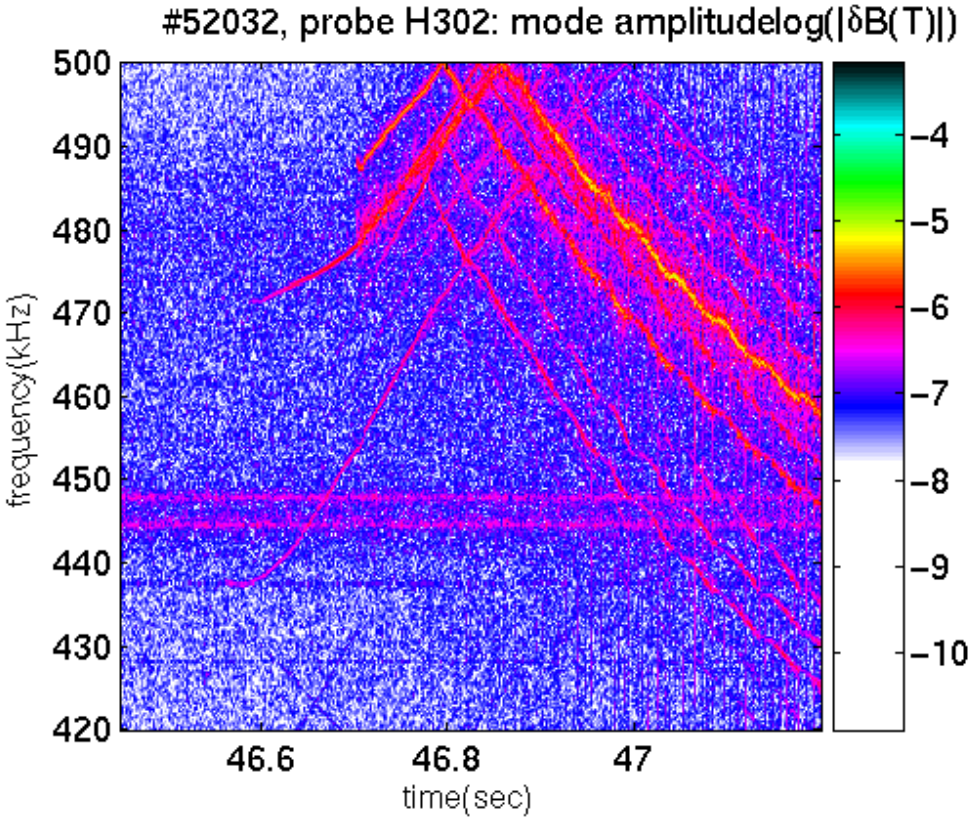

The mode "reflection" from the frequency boundary 500 kHz determined by 1MHz sampling rate of Mirnov coils on JET

THE NYQUIST UNDER - SAMPLING EFFECT IN PHASE

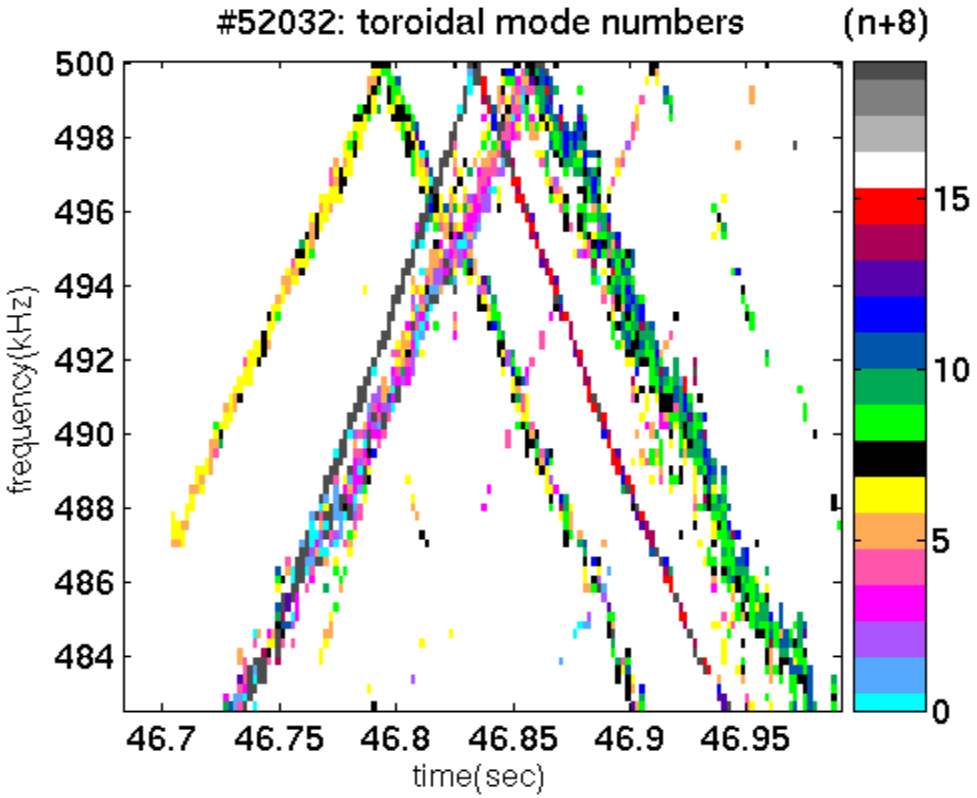

Toroidal mode numbers also experience a "reflection" n → (-n) from 500 kHz determined by 1MHz sampling rate of Mirnov coils on JET

DOPPLER SHIFT OF THE MODE FREQUENCY

- ***Uni-directional*** **NBI on JET drives a significant** ***toroidal plasma rotation*** **(up to f_{rot}~ 40 kHz)**

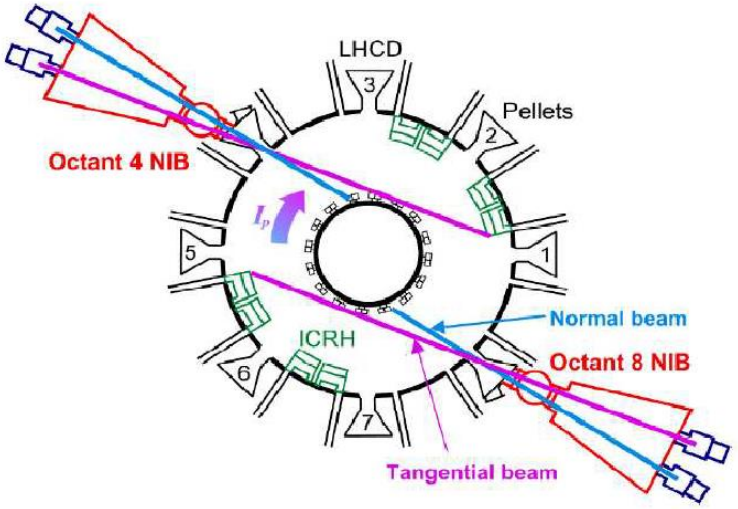

Geometry of NBI injection system on JET (view from the top of the machine)

- **Frequencies of waves with mode number n in laboratory reference frame, f_n^{LAB}, and in the plasma, f_n^0, are related through the Doppler shift $nf_{rot}(r)$:**

$$f_n^{LAB} = f_n^0 + nf_{rot}(r)$$

TAKING INTO ACCOUNT THE DOPPLER SHIFT WE CAN NOW COMPARE THE COMPUTED VERSUS OBSERVED TAEs

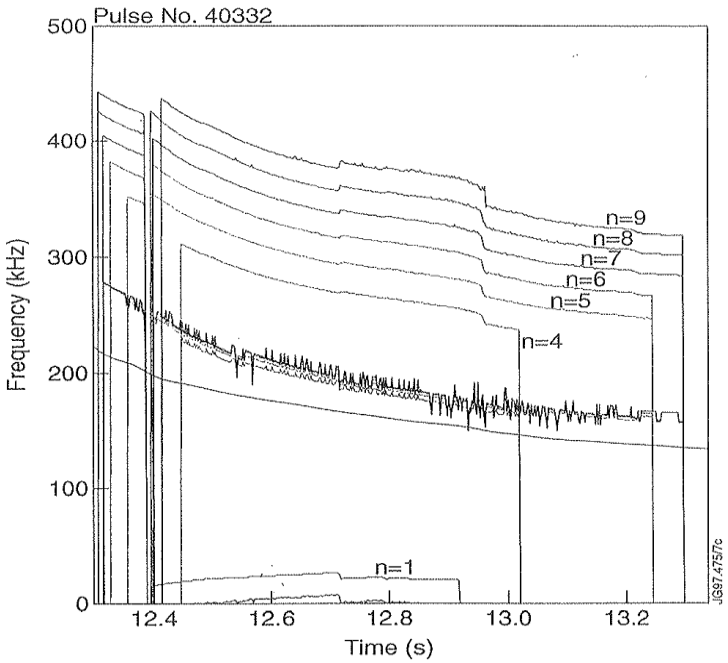

Eigenfrequencies of TAEs with n=4…9 computed for equilibrium in JET discharge #40332. Added Doppler shift matches the experiment

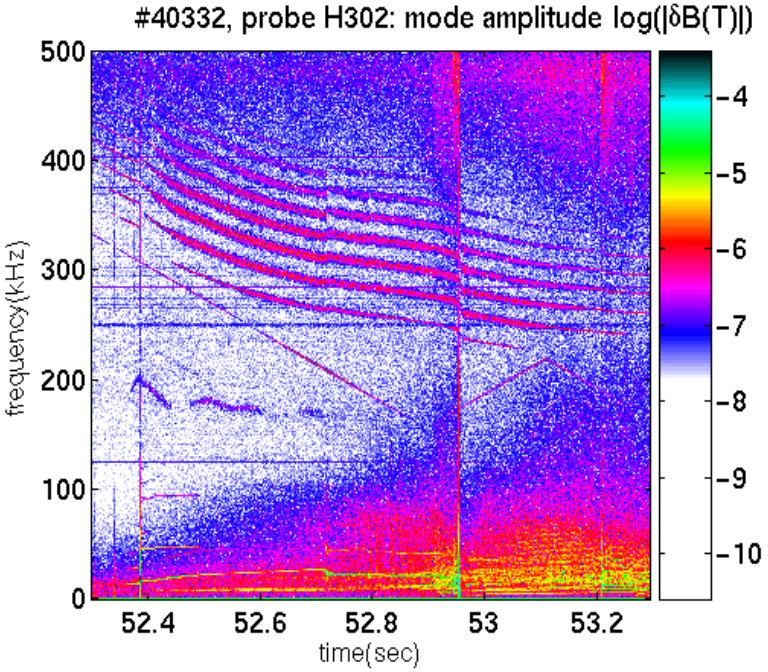

Discrete spectrum of TAE observed in JET discharge #40332. Plasma starts at t=40 sec. Frequency changes due to plasma density increase, $f \sim B/\sqrt{n_i M_i}$.

NEAR-THRESHOLD DYNAMICS OF TAE IN THE “SOFT” INSTABILITY CASE

GRADUAL INCREASE OF ICRH POWER FOR ICRH-DRIVEN TAE

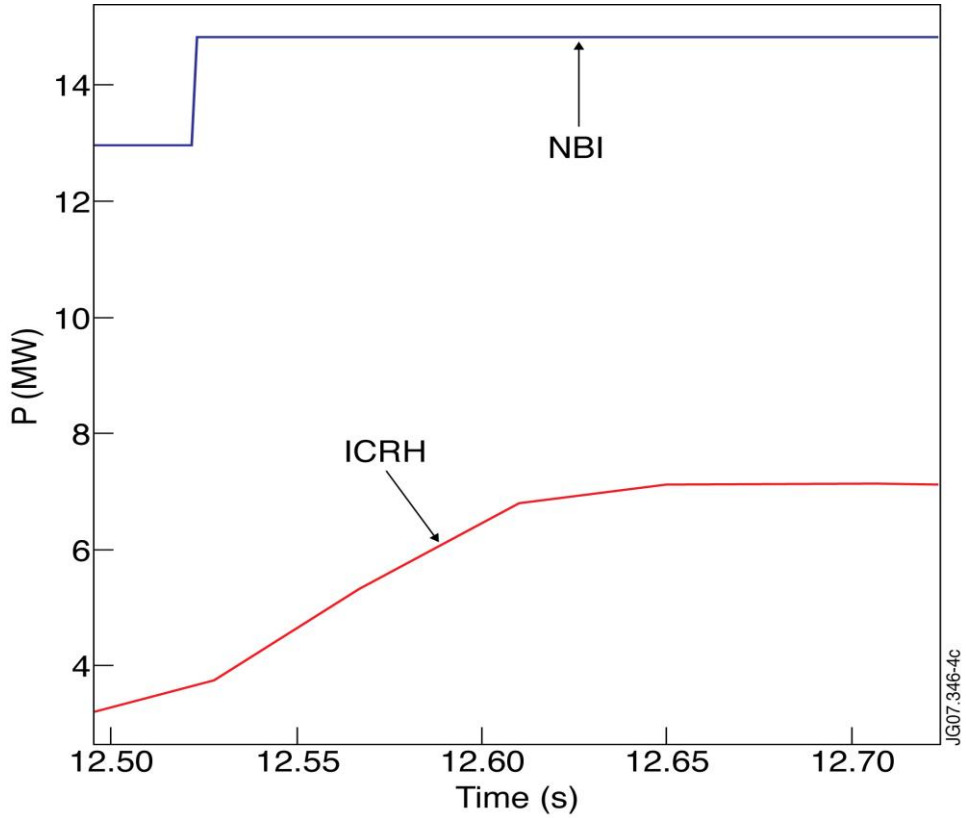

- **Power waveforms of ICRH driving TAE and NBI (NBI provides damping)**

EXPERIMENTALLY OBSERVED ICRH-DRIVEN TAE

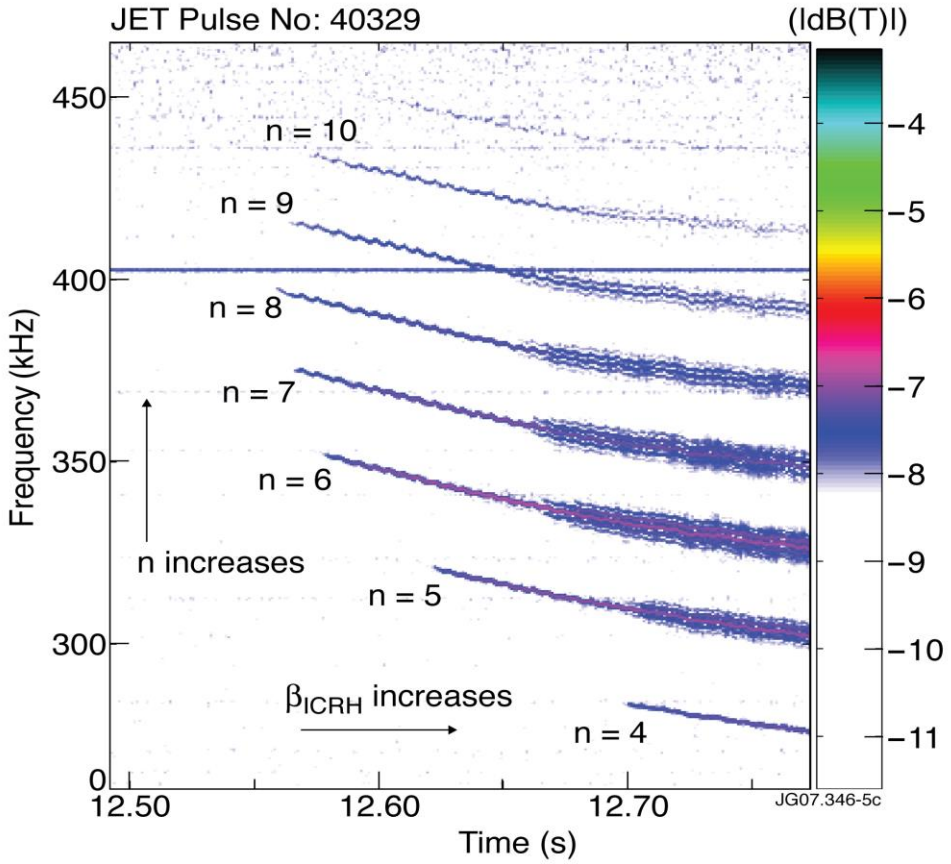

EXPERIMENTALLY OBSERVED TAE – QUESTIONS TO ASK

- **TAE frequencies are well above the expected 160 kHz. Why? Doppler shift**
- **TAE modes with $n = 6 - 9$ are excited easily, while TAE modes with lower or higher n's need a higher pressure of fast ions. Why? Stability depends on n**
- **The TAE spectral lines broaden and split after some time. Why? Nonlinear amplitude modulation becomes important**

LINEAR STABILITY OF TAE

- **In the presence of interacting fast ions, the solution for TAE in the form**

$$\phi(r,\vartheta,\zeta,t) = \exp\left(-i\omega\ t + in\zeta\right) \sum_m \phi_m(r)\ \exp\left(-im\vartheta\right) + c.c.$$

gets additional factor

$$\phi(r,\vartheta,\zeta,t) \to \phi(r,\vartheta,\zeta,t)\cdot\exp\left(\gamma\ t\right)$$

- **The exponential growth/ damping rate of TAE amplitude is determined by**

$$\gamma = \frac{P_\alpha - P_d}{2\cdot\delta W} \equiv \gamma_\alpha - \gamma_d$$

where P_α is power transfer from the energetic particles to the wave, P_d is wave power absorbed by background plasma, and δW is the wave energy given by the sum of field energy and kinetic energy due to $\delta E \times B_0$ drift:

$$\delta W = \int d\zeta d\vartheta dr \cdot Rr\left(\frac{\delta B_\vartheta^2}{8\pi} + \frac{\omega^2}{k_\parallel^2 c^2}\cdot\frac{\delta B_\vartheta^2}{8\pi}\right)$$

- **The mode is *linearly stable* when $\gamma = 0$.**

FAST PARTICLE DRIVE: QUALITATIVE PICTURE - 1

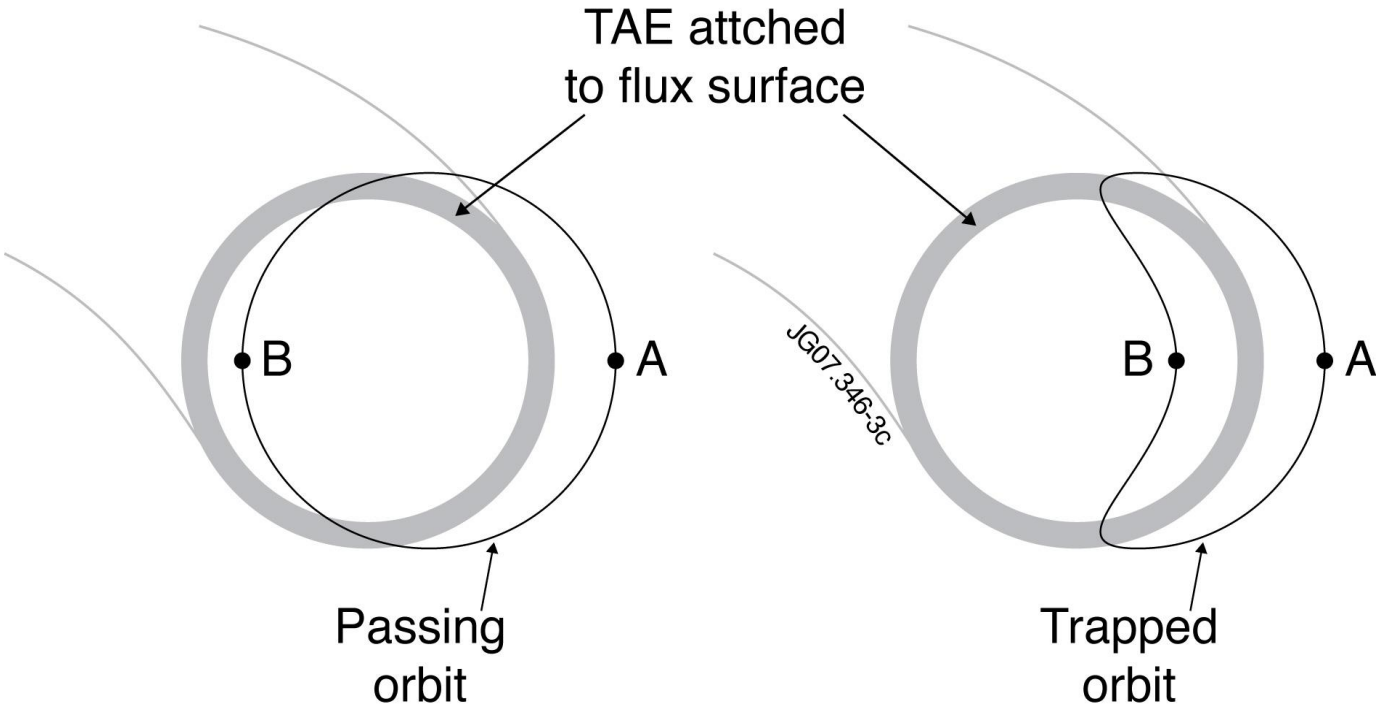

- **TAE modes are attached to magnetic flux surfaces, while the resonant ions are NOT! They experience drift across the flux surfaces and TAE mode structure**

FAST PARTICLE DRIVE: QUALITATIVE PICTURE - 2

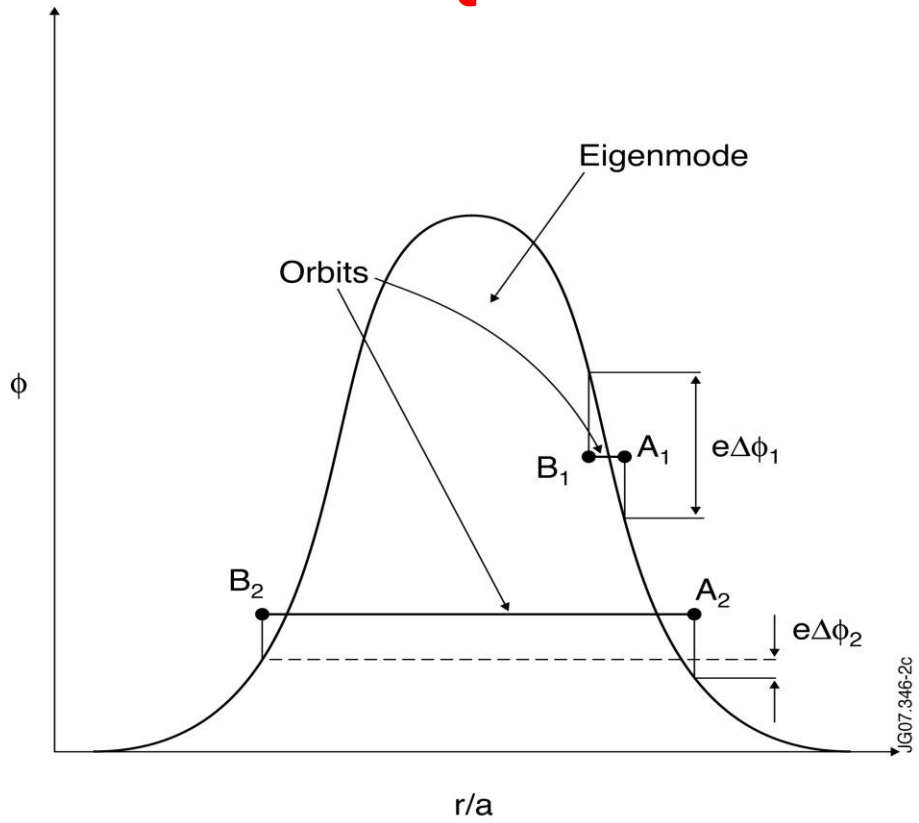

- **When resonant ion moves radially across TAE from point A to point B, the mode and the ion exchange energy $e\Delta\phi$ as Figure shows.**

FAST PARTICLE DRIVE: QUALITATIVE PICTURE - 3

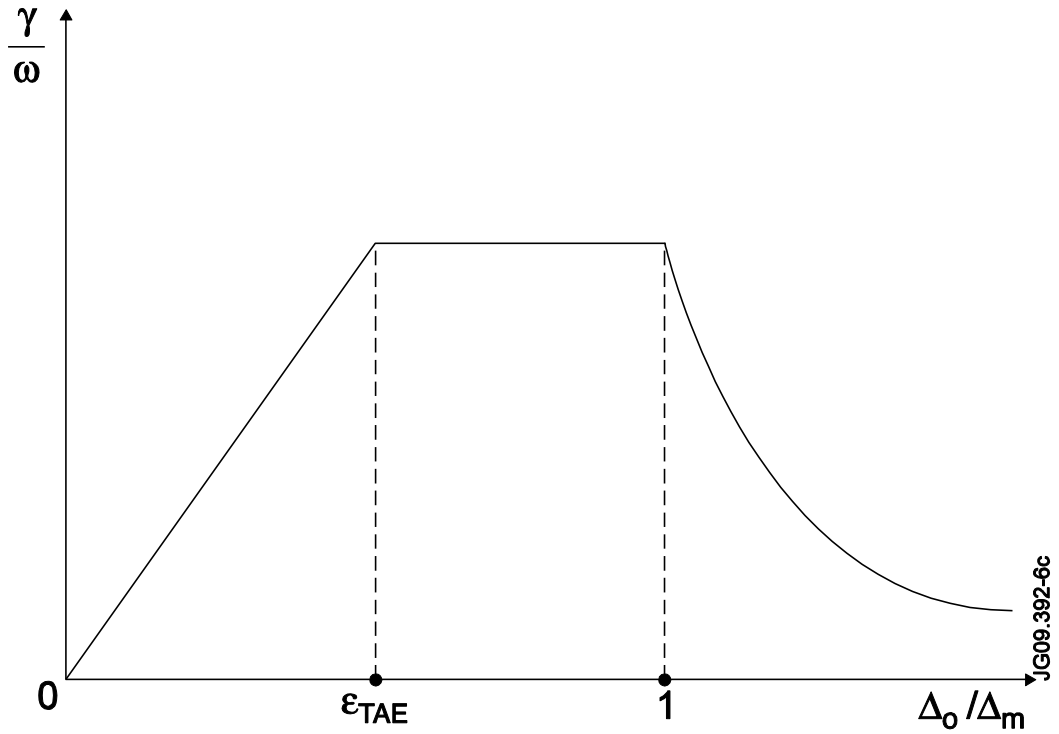

- **The maximum of $e\Delta\phi$ occurs when the orbit size, Δ_{orbit}, is equal to the mode width, $\Delta_{TAE} \approx r_{TAE}/m$, where m is poloidal mode number. This is why energetic ion drive is expected to have a maximum at $m \approx nq \approx r_{TAE}/\Delta_{orbit}$.**

POWER TRANSFER FROM ENERGETIC PARTICLES TO WAVE

- **Within the guiding centre approximation, the general expression is**

$$P_\alpha = \int d\zeta d\vartheta dr \cdot Rr \int d^3 v \left(-e_\alpha \mathbf{V_d} \cdot \delta\mathbf{E}\right) \cdot f$$

where $\mathbf{V_d}$ is the unperturbed guiding center drift velocity, and f is the linear perturbation of the guiding centre distribution function.

- **Assume for simplicity that (*Berk et al., Phys. Lett. A 162, p.475, 1992*)**

$$\omega << \omega_{*\alpha} = -\frac{m}{r} \cdot \frac{cE_\alpha}{e_\alpha B_0} \cdot \left(\frac{1}{p_\alpha} \frac{dp_\alpha}{dr} \right)$$

so that drift equation for *passing ions* is ($\Psi = n\varphi - m\vartheta - \omega t, \;\; \dot{\varphi} = v_\parallel / R, \;\; \dot{\vartheta} = v_\parallel / qR$ **)**

$$\frac{\partial f}{\partial t} - V_d \sin\vartheta \frac{\partial f}{\partial r} - V_d \cos\vartheta \frac{1}{r}\frac{\partial f}{\partial \vartheta} + \dot{\varphi}\frac{\partial f}{\partial \varphi} + \dot{\vartheta}\frac{\partial f}{\partial \vartheta} = \frac{c}{B}\left(1 - \frac{k_\parallel v_\parallel}{\omega}\right)\frac{1}{\bar{r}}\frac{\partial f_0}{\partial \bar{r}}\left(-im\phi_m + \frac{\partial \phi_m}{\partial \vartheta}\right)\exp\left(i\Psi_m\right) + c.c.$$

TAE FIELD IN THE ORBIT REFERENCE FRAME

- **Equation for drift orbit of the passing ions is**

$$r = \bar{r} + \Delta_O \cos\bar{\vartheta}\,, \qquad \vartheta = \bar{\vartheta} - \frac{\Delta_O}{\bar{r}}\sin\bar{\vartheta} \approx \bar{\vartheta}$$

- **The change of variables** $(r,\ \vartheta) \to (\bar{r},\ \bar{\vartheta})$ **meaning the transform to the orbit reference frame gives then**

$$\frac{\partial}{\partial r} = \frac{\partial}{\partial \bar{r}}\,; \quad \frac{\partial}{\partial \vartheta} = \Delta_O \sin\bar{\vartheta}\,\frac{\partial}{\partial \bar{r}} + \frac{\partial}{\partial \bar{\vartheta}}\,, \text{ so}$$

$$\frac{\partial f}{\partial t} + \dot{\varphi}\frac{\partial f}{\partial \varphi} + \dot{\vartheta}\frac{\partial f}{\partial \vartheta} = \frac{c}{B}\left(1 - \frac{k_\parallel v_\parallel}{\omega}\right)\frac{1}{\bar{r}}\frac{\partial f_0}{\partial \bar{r}}\left(-im\phi_m + \frac{\partial \phi_m}{\partial \vartheta}\right)\exp\left(i\Psi_m\right) + c.c.$$

where

$$\phi_m\left(\bar{r} + \Delta_O\cos\vartheta\right) = \sum_{l=0}^{\infty}\phi_{m,l}\cos l\vartheta$$

POWER TRANSFER FROM ENERGETIC PARTICLES TO WAVE

- **One obtains then for the resonance contribution**

$$f = -\frac{c}{2B\omega}\frac{1}{\bar{r}}\frac{\partial f_0}{\partial \bar{r}}\sum_l (m+l)\left(\dot{\Psi}_m \phi_{m,l} + \dot{\Psi}_{m+1}\phi_{m+1,l}\right)(-i\pi)\delta\left(\omega - n\dot{\varphi} + (m+l)\dot{\vartheta}\right)\exp\left[i\left(\Psi_m - l\vartheta\right)\right] + c.c.$$

- **NOTE that the resonance contributions are coming from**

$$v_{\parallel} = \frac{V_A}{|1-2l|}$$

- **The power transfer is then given by**

$$P_\alpha \propto -\beta'_\alpha \frac{c^2}{\omega}\left(\frac{V_A}{V_0}\right)^{p+1}\left(\frac{\Delta_O}{\Delta_{TAE}}\right)^{p-1}\sum_l \frac{(m+l)}{|1-2l|^{p+2}} C_l^p \left(\frac{v_{crit}}{V_A}|1-2l|\right)^{2p-1}$$

where p =1, 2 for large and small orbit widths correspondingly

TAE DAMPING EFFECTS

- **Thermal ion Landau damping is given by**

$$\frac{\gamma_i}{\omega} \cong -\frac{\pi^{1/2}}{4}\beta_i q^2 \lambda_3 \left(1+\left(1+2\lambda_3^2\right)^2\right)\exp\left(-\lambda_3^2\right), \quad \lambda_3 = 1/9\beta_i$$

- **Electron Landau damping is small, the main electron damping comes from Coulomb scattering**

$$\frac{\gamma_e}{\omega} \cong -\left(\frac{\nu_e}{\omega}\right)^{1/2}\left(4\beta_e q^2 + 0.44\left(\frac{\rho_S}{\Delta_{TAE}}\right)^2\right)\cdot\left(\ln\left[16\left(\frac{\varepsilon\omega}{2\nu_e}\right)^{1/2}\right]\right)^{-3/2}$$

- **Some continuum damping isstill possible if the radial "tail" of TAE intersects the Alfvén continuum structure**

- **Small but finite coupling of TAE to Kinetic Alfvén Waves leads to TAE energy radiated away in radius – this effect is called radiative damping.**

TAE EXCITATION EXHIBITS DEPENDENCE ON MODE NUMBER

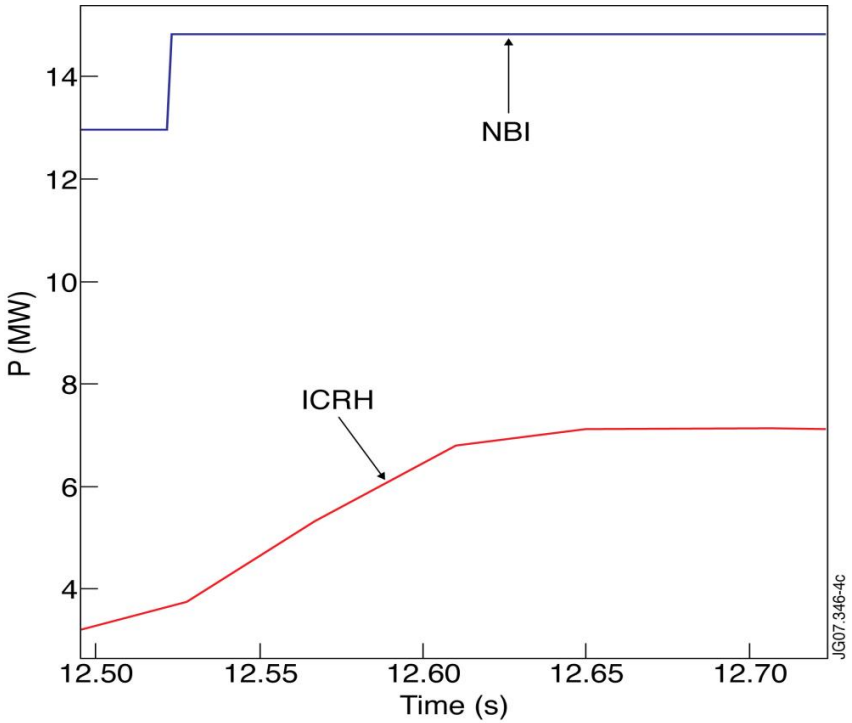

Power waveforms of ICRH driving TAE and NBI (NBI provides damping)

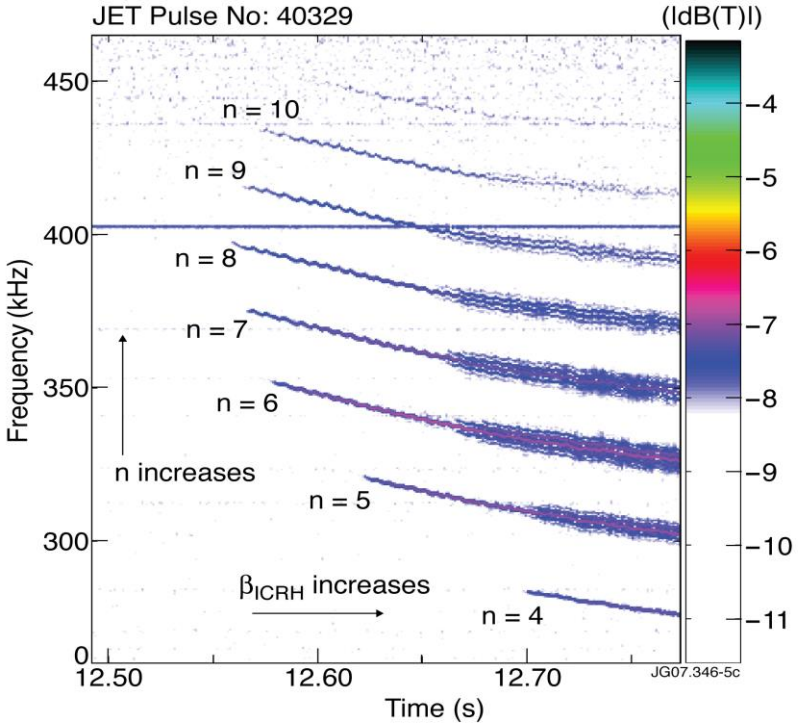

TAEs with toroidal mode numbers from n=4 to n=10 are seen separated by frequency ~ 25 kHz

STABILITY OF α-PARTICLE DRIVEN TAE IN JET DT DISCHARGES

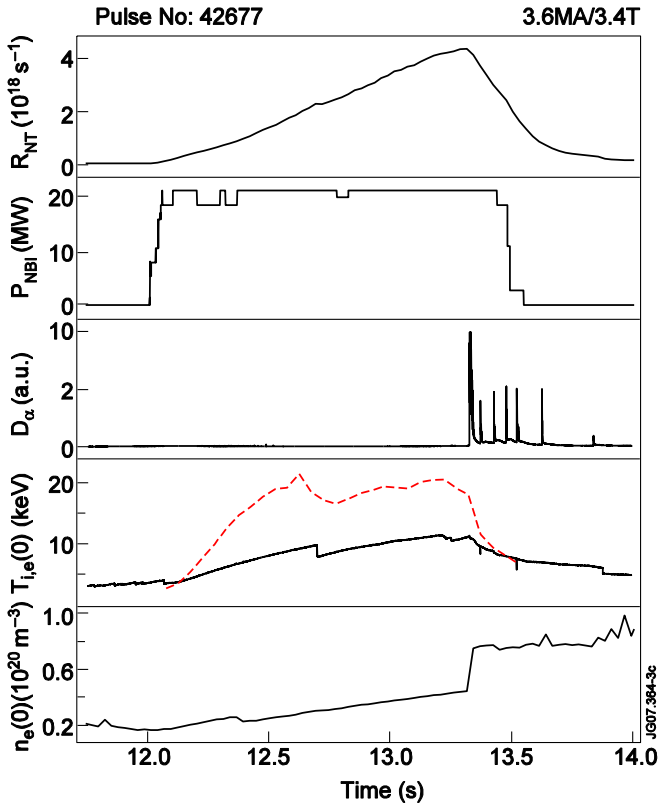

Temporal evolution of the DT fusion rate, NBI power, D_α signal, central ion (broken line) and electron (solid line) temperatures and central electron density in DT discharge #42677 in JET (1997)

TAE STABILITY IN JET DT DISCHARGES - 2

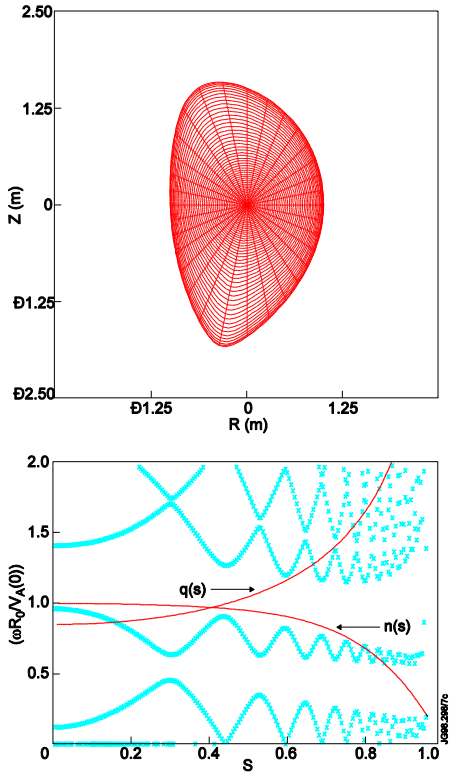

The reconstructed equilibrium for DT discharge #42677 at t = 13.3 sec together with the Alfvén continuum structure. q(s) and n(s) are the safety factor and electron density radial profiles; q(0) = 0.85.

TAE STABILITY IN JET DT DISCHARGES - 3

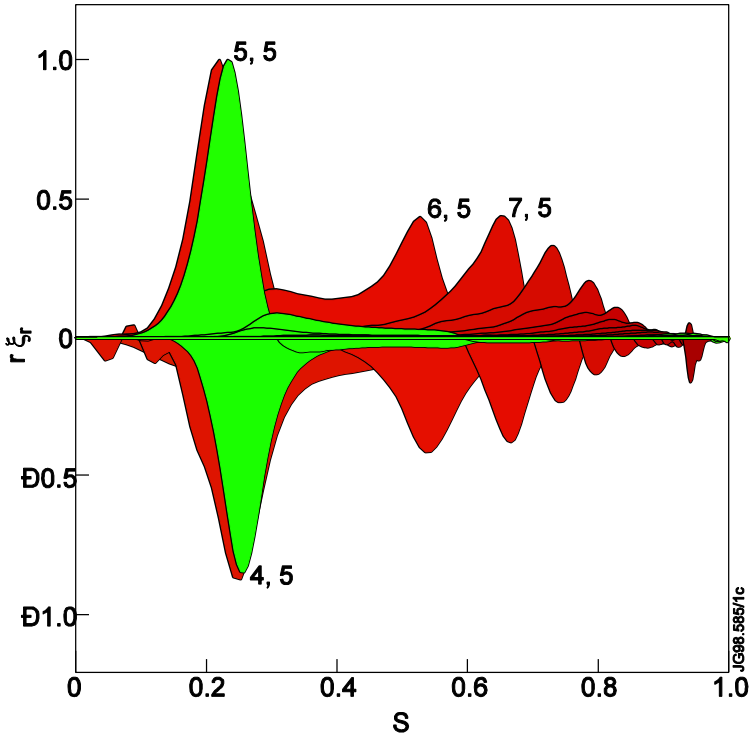

The computed TAE (red colour) with eigenvalue in the DT discharge #42677 at t = 13.3 sec. In addition, the most unstable upper core localised TAE analysed in the modelling prior to the DT experiments is shown (green colour or grey in black-and-white).

TAE STABILITY IN JET DT DISCHARGES - 4

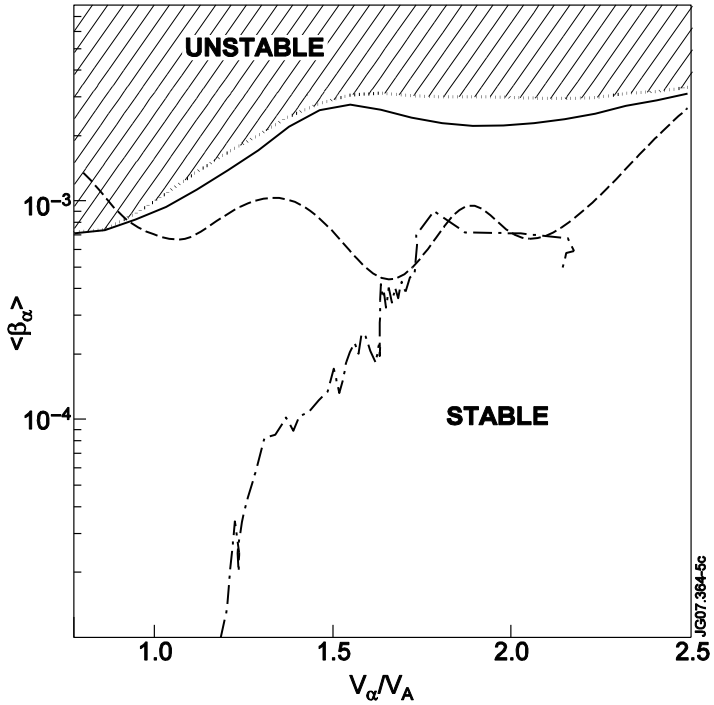

The instability zone (tinted) computed by the CASTOR-K code for alpha-particle driven TAEs shown in previous Figure. The instability boundary for the upper core localised TAE is also shown for comparison (dashed curve). The actual path of the parameters in discharge 42677 is computed by the TRANSP code and is marked by the chain curve.

TAE STABILITY IN ITER-94 (α-particles only)

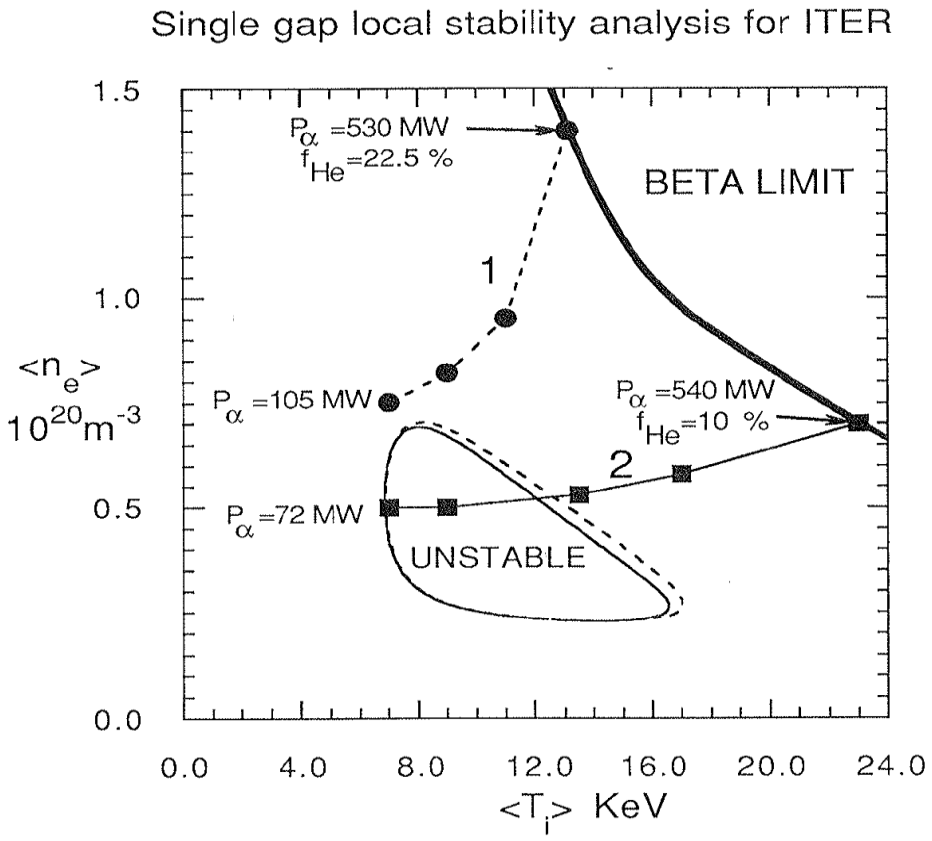

SUMMARY

- Linearised ideal MHD equations describe *compressional Alfvén, slow magnetosonic, and shear Alfvén waves*
- In shear Alfvén wave the fluid displacement vector ξ and $\tilde{\mathbf{E}}$ are perpendicular to the magnetic field $\mathbf{B}_0$. The wave propagates along $\mathbf{B}_0$: $\omega = \pm k_{\|} V_A$
- In inhomogeneous plasma, shear Alfvén wave experiences strong continuum damping
- In cylindrical plasma with current, a discrete eigenmode may exist, Global Alfvén Eigenmode, which has no continuum damping
- In toroidal plasma, the coupling between poloidal harmonics give TAE-gaps in Alfvén continuum and may give TAE-modes that have no continuum damping
- TAEs driven by energetic particles are often seen in present-day machines and their linear theory is in a good agreement with the observations